TECHNICKÁ UNIVERZITA V LIBERCI
Fakulta strojní

Design of a Fire Pump

Diplomová práce

Studijní program: N2301 – Mechanical Engineering
Studijní obor: 2302T010 – Machines and Equipment Design

Autor práce: **Ahmad Ajami**
Vedoucí práce: doc. Ing. Václav Dvořák, Ph.D.

Liberec 2019

TECHNICAL UNIVERSITY OF LIBEREC
Faculty of Mechanical Engineering

Design of a Fire Pump

Master thesis

Study programme: N2301 – Mechanical Engineering
Study branch: 2302T010 – Machines and Equipment Design

Author: **Ahmad Ajami**
Supervisor: doc. Ing. Václav Dvořák, Ph.D.

Liberec 2019

TECHNICKÁ UNIVERZITA V LIBERCI
Fakulta strojní

Zadání diplomové práce

Design of a Fire Pump

Jméno a příjmení:	**Ahmad Ajami**
Osobní číslo:	S17000372
Studijní program:	N2301 Mechanical Engineering
Studijní obor:	Machines and Equipment Design
Zadávající katedra:	Department of Power Engineering Equipment
Akademický rok:	**2018/2019**

Zásady pro vypracování:

1. Performe literature review of design of centrifugal pumps, focus on fire pumps. Compile at least 10 references.
2. Measure characteristic of existing fire pump and obtained data put into dimensionless coordinates. Compare results with simple 1D computation and numerical computations.
3. Identify weaknesses of existing desing and suggest improvements. Perform numerical investigation of the new design and compare it with the existing one. Present new desing in suitable form.
4. Analyse results and compile conclusions.

Rozsah grafických prací:	10 stran
Rozsah pracovní zprávy:	40 stran
Forma zpracování práce:	printed
Jazyk zpracování práce:	English

Seznam odborné literatury:

[1] GÜLICH, Johann F. *Centrifugal pumps.* Springer, 2010.

[2] KARASSIK, Igor J. *Engineers' guide to centrifugal pumps.* McGraw-Hill, 1964.

Vedoucí práce:	doc. Ing. Václav Dvořák, Ph.D. Department of Power Engineering Equipment
Datum zadání práce:	1 November 2018
Předpokládaný termín odevzdání:	30 April 2020

prof. Dr. Ing. Petr Lenfeld
Dean

Technická univerzita v Liberci
-8-

doc. Ing. Václav Dvořák, Ph.D.
Head of Department

Liberec 1 February 2019

Declaration

I hereby certify I have been informed that my master thesis is fully governed by Act No. 121/2000 Coll., the Copyright Act, in particular Article 60 – School Work.

I acknowledge that the Technical University of Liberec (TUL) does not infringe my copyrights by using my master thesis for the TUL's internal purposes.

I am aware of my obligation to inform the TUL on having used or granted license to use the results of my master thesis; in such a case the TUL may require reimbursement of the costs incurred for creating the result up to their actual amount.

I have written my master thesis myself using the literature listed below and consulting it with my thesis supervisor and my tutor.

At the same time, I honestly declare that the texts of the printed version of my master thesis and of the electronic version uploaded into the IS STAG are identical.

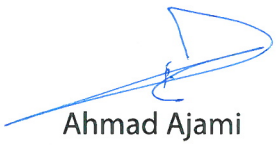

3. 5. 2019

Ahmad Ajami

Acknowledgment

First of all, I would like to thank who sacrificed their life for giving me and my brothers a prosperous and happy life, **my dear Parents**. I appreciate that gratefully and I wish them a long life with health and wellness.

I would like to express my gratitude to my supervisor doc. **Václav Dvořák** the head of our department (power engineering equipment) for his useful comments, remarks and engagement through the learning process of this master thesis. The door to Prof. Dvořák's office was always opened to me whenever I ran into a trouble spot or had a question about my research or writing.

I express my gratitude to the Czech Government and send them my regards for giving me this great chance. Without the scholarship, I wouldn't be writing this thesis. I have experienced a lot in the past two years that substantially changed my perspective on life.

I would like to dedicate my success to my first home **Syria** and I want to thank all the people there who wished me success in my life even in a small issue and all people who wished me a prosperous life, and I would like to thank you all for that. In addition I hope that **Syria** will return safely and have a happy life conditions.

In addition, I would like to thank dr. **Müller**, dr. **Vestfálová** and all our department staff for their help, support and all other consultations that I needed during my study.

Also I would like to send my regards to Mr. **Tomáš Váňa** and Mr. **Pavel Pavliš** from Pavliš & Hartmann company for their help during my experiment and wish them a successful life.

Finally, I am grateful to my friends who were standing beside me during my study whatever moments sweet or bitter, I particularly mention Mr. **Anas Elbarghthi**, Mr. **Gafaru Moro**, Miss. **Myka Duran** and all other colleagues who spent last two years together.

Ahmad Ajami

Nomenclatures

Symbol	Unit	Description
η	%	efficiency
η_v	%	Volumetric efficiency
η_H	%	Hydraulic efficiency
H	m	Pump head
Q_{out}	m^3/s	Useful flow rate
N_s	rpm	Specific speed
β_1	deg	Inlet blade angle
β_2	deg	Outlet blade angle
b_1, b_2	mm	Impeller width at inlet and outlet
N	rpm	Impeller speed
ρ	Kg/m^3	density
μ_{eff}	Pa/s	Dynamic viscosity
U_1, U_2	m/s	Impeller speed at inlet and outlet
$\mathbf{C_{m3}}$	m/s	Absolute velocity's projection
$Q_{N,}$	m^3/s	Nominal flow rate
H_N	m	Nominal Pump head
G_b	m^2/s^2	Generated turbulence kinetic energy due to the buoyancy
G_k	m^2/s^2	Generated turbulence kinetic energy due to the velocity gradients
K	m^2/s^2	Turbulent kinetic energy
P_{in}	Pa	Total inlet pressure
P_{out}	Pa	Total outlet pressure
ΔP_d	W	Disk friction losses
P_e	W	Hydraulic power
P_l	W	Impeller power
M	N.m	Torque
ω	rad/s	Angular velocity
C_{in}, C_{out}	m/s	Absolute velocity at inlet and outlet
ψ	-	Head coefficient
φ	-	Flow rate coefficient
χ	-	Power coefficient
ξ		Relative roughness coefficient
Re	-	Reynolds number
ε	mm	Wall roughness
D	mm	Impeller diameter
C_{2u} C_{1u}	m/s	Absolute velocity's projections
Y_L	W	Specific work
Y	W	Provided power
Q_l	m^3/s	Leakage flow rate
Q_E	m^3/s	Balancing flow rate
Q	m^3/s	Total flow rate
P_{losses}	W	Mechanical Losses

P	W	Total power
P_{dyn}	Pa	Dynamic pressure
P_{hyd}	W	Hydraulic power
Ψ	-	Dimension less head pump
Ω	-	Dimension less flow rate
P_a	Pa	Inlet pump pressure
P_v	Pa	Vapor pressure
h_{fs}	m	Hydraulic losses

Shortcuts

Superscripts	description
NFPA	National Fire Protection Association
BHP	Break horse Power
BEP	Best Efficiency Point
$NPSH_a$	Available net positive suction head
$NPSH_r$	Required net positive suction head

Table of Contents

Abstract

Nowadays, most research on pump design are focused on the efficiency of pump and solving its problems, but a few of researchers focus on the fire pump machine a, whatever if hydraulic or design view, because in the fire pump engine, the efficiency isn't that much important, where in fire pump the important parameters are flow rate and the head of the pump regardless its efficiency. Nevertheless, the fire pump needs high capacity for operation process to provide the required flow rate at the required head so that the pump performance can be enhanced. One of the influencing phenomena is the cavitation inside the pump structure, especially at high operating speed where there is a huge vacuum created for sucking water and pumped later. In this study, the pump characteristic of a firefighting pump was calculated by an experiment and by a numerical simulation too. In addition, cavitation presence was investigated in order to compare it with the experiment results too.

Introduction

As known by researchers in the field of machine design, the efficiency of every machine is the main aim and the first motivation for advance research. The field of turbo machinery is no exception, and therefore, many designers carry out research to improve the efficiency of turbo machines.

Pump designs often rely on experiments, calculation, simulation and comparison between previous and present study. Nowadays, most of the research are done by computational fluid dynamic CFD, where this method has many advantages like stability, prediction the accurate results, fast, showing contours, drawing diagrams, non-destructive of the machine, and flexibility in terms of changing input parameters.

At the outlet of the impeller of the pump, the internal flow characterized by complexity due to circumferential distortion caused by asymmetry of the shape of volute around the rotor, especially at non-nominal conditions (design-off condition). Moreover, the interaction between the impeller-spiral curves causes more dynamic effect that influences the total pump efficiency. The non-nominal operation conditions, dynamic effect and particularly the pressure field lead to unbalance of the radial forces.

However, the studies of the main influencing parameters on the pump manufacturing are available at open literature. **Kergourlay et al. [3]** Tested the influence of increasing the splitter curve in a hydraulic centrifugal pump rotor, where the comparison of the impeller characteristic between two impeller with/without splitter curve was done. **Gonzalez et. [4]** Studied the influence of the outlet blade angle effect on the impeller performance. **K.M. Pandey [5]** Studied the effect of the blades number on pressure changes for 6 to 10 blades.

1. Fire pump design

1.1. Fire pump of optimal performance [1]

According to National Fire Protection Association NFPA, to achieve the requirement of the fire pump engine, the pump characteristic line must be in the green area between two limit curves as illustrated in Fig. 1:

- The head pressure of the pump at 150 % of the pump flow rate (at the secondary point) will be in the range from minimum of 65% of the rated head (primary head) to a maximum of just below the rated head.
- At shut off head where there is no flow rate, the head pressure will be from the minimum value 101% to the maximum value 140% of the rated head.
- The minimum head at 65% of rated head must be achieved when the has a 15 ft suction lift.

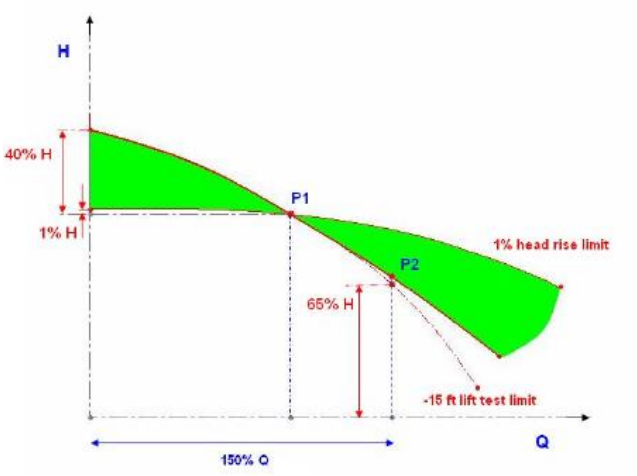

Fig.1: Performance requirements for fire pump head [1].

According the above constraints the secondary head is higher than the percentage of the primary head, where it follow that fire pump specific speed range of fire pumps is determined from upper curve, because at high speed of the pump the head curve would be too steep to meet the allowable curve. It is worth mentioning that at the secondary point if the head pressure is exactly 65 % the pump head must not be affected with 15 ft suction lift.

The required power for operating pump shaft (Break horse Power BHP), which matched with head curve in the green area in the Fig.1. where the BHP curve which agrees to the steeper head-capacity curve, it can be driven at lower input power at the right section thus, the required motor will be smaller. The lowest normalized break horse power limit against the specific speed is not known very well as the efficiency pump, and it has not determined yet.

1.2. Optimal Fire Pumps vs. Best Efficiency Pumps

The pump efficiency is an important parameter for design the most energy-saving pump **[1].** In the Fig. 2, there are two different efficiency curves for two different pumps against the flow rate, where it is not easy to know the better one without a knowledge of the operation conditions. Fig.2 illustrate two curves, where the most energy-saving pump perhaps related to the curve 1,

where its peak of the efficiency is less than that of curve 2. The best efficiency for the pump is the optimal energy-saving but, at different operation like flow rate, speed, and some other parameters cause different optimal efficiency pump.

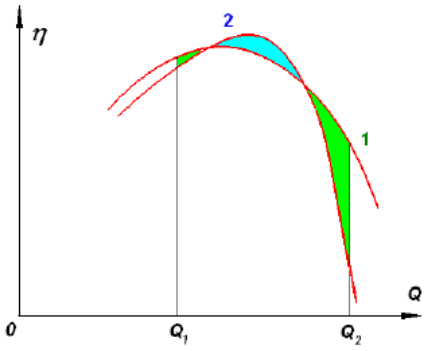

Fig. 2. Two efficiency curves of two different pumps [1].

In other words, and for more detailed explanation about the pump performance and how it differ between the efficiency pump and the optimal fire pump, the comparison of the normalized head and the break horse power was done across a range of specific speed N_s. Fig. 3 and 4. show the BHP and the non-dimensional head curves at different specific speed of the efficiency pump.

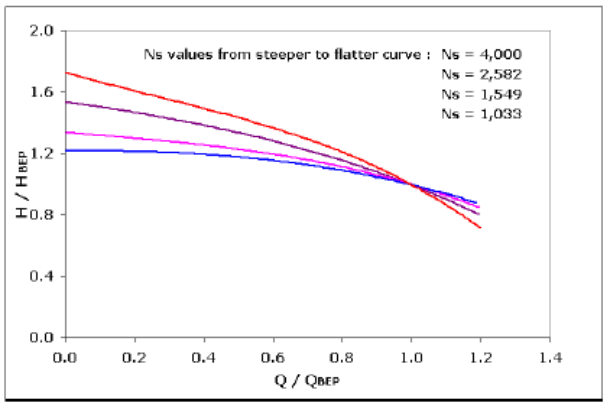

Fig.3: Non-dimensional head-capacity curves of best efficiency pumps [1].

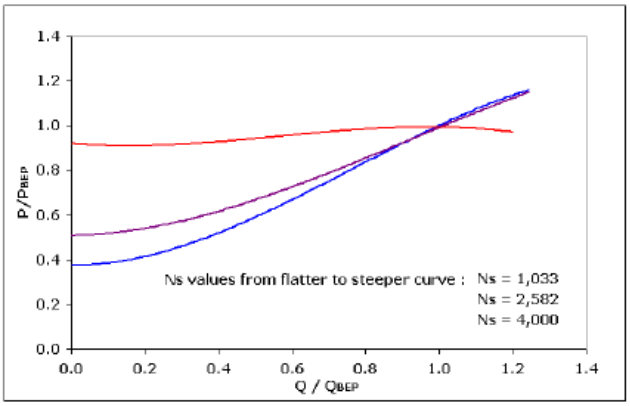

Fig.4: Non-dimensional power curves of best efficiency pumps [1].

The normalized head and BHP curves of best efficiency pumps at different specific speeds are shown in Fig. 3 and Fig. 4 respectively. As noted in the Fig. 4 the required power of the operation process increases with increasing the mass flow rate. Where, N_S: is specific speed, H/H_{BEP}: is non-dimensional head, Q/Q_{BEP}: is non-dimensional flow rate, P/P_{BEP}: is non-dimensional power. Fig.5 and Fig.6 illustrate the same characteristic, non-dimensional head and non-dimensional power vs. non-dimensional flow rate and what would be in the case of optimal fire pump at the same band of specific speed. As shown in the Fig. 6 the power stays almost constant at different specific speed beyond the best efficiency point. We can achieve the

downturn in the BHP because of the reserve of head at the secondary flow point, which allow to increase the steep of the head curve, reduce the power [1].

Note: all charts at specific speed range [1000, 5000]. The next equation is non-dimensional expression of the BHP (Break Horse Power):

Break Horse Power = (Head * Capacity) / Efficiency **(1)**

Where, "Capacity" and "Head" are normalized with respect to the best efficiency point (BEP) capacity and head, respectively. By introducing some design change, the head can be dropped to a larger range than the efficiency, thus BHP is reduced.

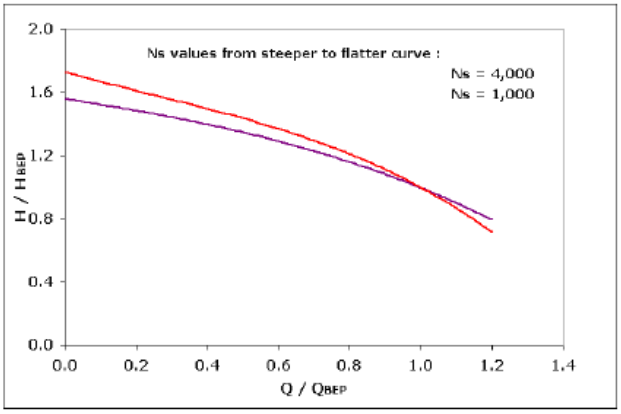

Fig.5: Non-dimensional head-capacity of the optimal fire pump [1].

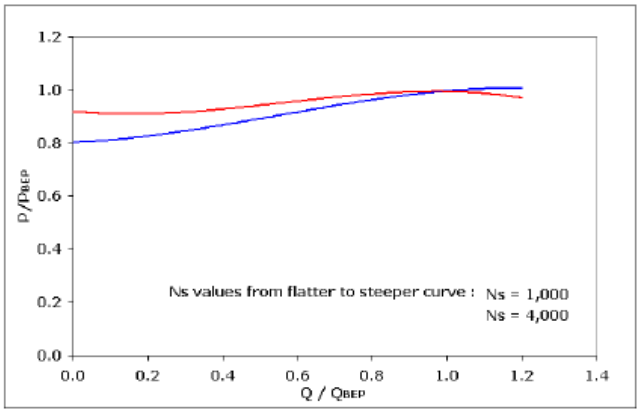

Fig.6: Normalized power curves of the best optimal fire pump [1].

Assuming a 45 degree slope of the normalized head curve around the best efficiency point, the break horse power is saturated at BEP due to the efficiency in the nearness of the BEP is almost constant. This was noted by **Sdano, 2009 [1].** Beyond the best efficiency point, the efficiency drops while the slope of the head curve decreases enough to cause the BHP curve slope to become negative and thus, the BHP will decrease. In other words, the criteria of 45 degree slope of the non-dimensional head curve at best efficiency point is a reasonable criterion for optimal fire pump at the high specific speeds in the range upper (below 4000).

At lower level of the specific speed, a fire pump can't have a steep head curve without sacrificing efficiency. For that reason, the optimal fire pump at the low specific speed don't necessarily to have a peak for break horse power curve at the best efficiency point. The lower the specific speed, means a larger in the deviation of the optimal fire pump design from the design of best efficiency pump (compare Fig. 3 vs. Fig. 5, and Fig. 4 vs. Fig. 6). This poses greater challenges in optimal fire pump design at lower specific speeds.

Now the question is " Is it possible for best efficiency pump to be used as an optimal fire pump?", **Stepanoff, A. J., (1957) [6],** that is possible in case there is no room to minimize the capacity of the best efficiency pump by modify the design without losing the lift test requirements. **Mr. Stepanoff** said, that may occurred just in narrow band of specific speed

around 4000 rpm where, best efficiency pumps at 4000 as specific speed have a maximum break horse power at the BEP.

1.3. Pump design and its cases according to outlet blade angle [2]

The reason of complexity in pumps, fans and other turbo machinery is primarily because of the three dimensional developed structures including unsteadiness, turbulence secondary flow and other parameters. Initially, pump design was based on some experiment and its correlations with testing and based on engineering experiences too. Nowadays, the designer base on their understanding of the internal flow, turbulence model, design/off-design conditions and the other phenomenon to design the model for getting the best efficiency by using computational fluid dynamic CFD to predict the flow and its parameters within the pump in order to improve its performance.

The complexity of the internal flow often appears a circumferential deviation because of the shape of the volute and the tongue, especially if the pump works at non ideal point (off-design point). In addition, the interaction between the rotor-volute causes dynamic effects which affect the pump efficiency. Mainly the non-uniform flow rate and the pressure field distribution create unbalance in the rotor which increase the centrifugal forces. All these parameters are very important for pump design view. Where there are many of researcher did some experiments and simulated many designs to know more about the pump design.

Bacharoudis, [2] studied the influence of outlet angle for a centrifugal pump and design it, where he worked with different outlet blade angle β_2 as 20, 30, 50 and then simulated them by Fluent software. The volute of the pump in the laboratory has a rectangular section shape with rounded corners and the diffuser extends in the radial direction.

Three shrouded rotors were used with constant width b=20 mm and with six untwisted backward blades facing, in addition the length of the blades, impellers diameters and the blade leading edge angle β_1=14 deg, were almost the same in all impellers, just the trailing edge angle β_2 was different as 20, 30 and 50 deg. The impeller diameters at the inlet and the outlet are respectively 150, 280 mm.

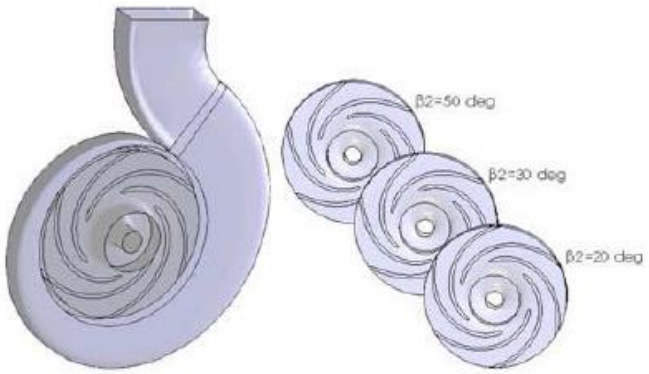

Fig.7: Laboratory pump with the three radial impeller [2].

At the impeller speed N= 925 rpm, the volumetric flow rate of the three impellers is 0.0125 m3/sec and based on the one dimensional theory the estimated pump's total head (H) is 10 m, that results in the value 18.4 for the specific speed (rotation speed of a pump which is similar to another pump that gives mass flow Q = 1 m^3/s for head H = 1 m). The hydraulic efficiency (transferred power into pumped fluid divided by the required power to operate the pump) of the centrifugal pump η_H at the operating point reaches its maximum value 0.83.

1.3.1. Governing equations

Inside the stationary and rotational parts of the pump the fluids flows, and for each part of the pump there are governing equations. Through the stationary parts the incompressible flow equations was solved in an inertia reference speed frame, and through the impeller was solved in a moving frame of reference with constant speed.

The governing equations for the impeller are formulated as continuity and momentum equations. (2) and (3), the governing equations for the stationary parts are formulated continuity and momentum equations. (2) and (4), as follow:

$$\nabla \rho u_r = 0 \tag{2}$$

$$\nabla \rho u_r + 2\rho\Omega * u_r + \rho\Omega * \Omega * r = -\nabla \mathrm{p} + \mu_{eff} \nabla^2 u_r \tag{3}$$

$$\nabla \rho \mathrm{u} = -\nabla \mathrm{p} + \mu_{eff} \nabla^2 u \tag{4}$$

Where **ρ** is the density of the fluid, **Ω** is the rotational speed and $\boldsymbol{\mu_{eff}}$ is the dynamic effective viscosity, **p** is the static pressure, $\mathbf{U_r}$ is the vector fluid velocity in the rotating system, **U** is the vector fluid velocity in the stationary frame reference.

The model **K- ε** was used as a turbulence model which is rated as most used model, that combine reasonable accuracy, robustness and simplicity. On the other hand, the model has been tested for different industrial flow and it shows identical results. The differential transport equations for the turbulence dissipation rate and the turbulence kinetic energy are:

$$\nabla \rho u k = \left(\left(u + \frac{u_t}{\sigma_k} \right) \nabla \mathrm{k} \right) G_k - \rho\varepsilon \tag{5}$$

$$\nabla \rho \mathrm{u} \varepsilon = \left(\left(u + \frac{u_t}{\sigma_\varepsilon} \right) \nabla \varepsilon \right) + C_{1\varepsilon} \frac{\varepsilon}{k} G_k + C_{2\varepsilon} \rho \frac{C^2}{k} \tag{6}$$

$$u_t = \rho c_m \frac{k^2}{\varepsilon} \tag{7}$$

Where, **u** is the local velocity vector, **k** is the turbulent kinetic energy, $\mathbf{G_k}$ represents the generation of turbulent kinetic energy due to the mean velocity gradients, **ε** is the dissipation rate, **μ** is the laminar viscosity, $\boldsymbol{\mu_t}$ is the turbulent viscosity, $\boldsymbol{\sigma_\varepsilon}$ and $\boldsymbol{\sigma_k}$ are the turbulent Prandtl numbers and $\mathbf{C_{1\varepsilon}}$=1,44, $\mathbf{C_{2\varepsilon}}$=1,92 and $\mathbf{C_m}$=0,09 are the constants of the model [2].

1.3.1.1. Computational issues

1.3.1.1.1. Geometry and mesh

The spatial discretization was applied for the flow domain in the numerical simulation of the radial pump. Neglecting of the all gabs between the impeller, volute and the pump case was done in the current simulation. All model includes three sub-zones. The second one is moving which presents the impeller at 925 rpm, the first and the third one present the stationary zones which are the inlet and the volute zones. As mentioned above, the first zone is the inlet pipe with 50 mm radius, the third zone is the volute zone or the outlet portion where the flow will be already developed with no reaction of outlet boundary conditions. The second domain is the intermediate one which consists the pump rotor. There are additional faces inside the model which separate all zones by forming different blocks. By this method the cell quality and density in local is more suitably controlled and handled depending on velocities and pressure gradients.

1.3.1.1.2. Numerical results

The pump characteristic for different outlet blade angle of three rotors is correlated by the H-Q curve slope for all rotors. The shape of H-Q curve becomes flatter and more smooth when the outlet blade angle increases, this relation is illustrated by the equation below:

$$H = \mu.\eta_H.\frac{u_2^2}{g}.\left(1 - \frac{c_{m3}}{u_2}.cot\,\beta_2\right) \quad (8)$$

Where, $\boldsymbol{\eta_H}$ is the hydraulic efficiency, $\boldsymbol{\mu}$ is the slip factor, $\mathbf{C_{m3}}$ is the meridian velocity at the exit of impeller passage, $\mathbf{U_2}$ is the peripheral velocity at the outlet section of the impeller and $\boldsymbol{\beta_2}$ is the outlet blade angle.

Equation. (8) shows the influence of the parameters (C_{m3}/U_2 and β_2) on the total head. In case of reduction the ratio C_{m3}/U_2 the total head rate will increase, in contrast when the outlet blade angle increase the total head increase too. Nevertheless, the influence of that angle is almost cancelled because the slip factor formulas show that larger angle β_2 leads to decrease the value of slip factor, which affects the H-Q curve shape

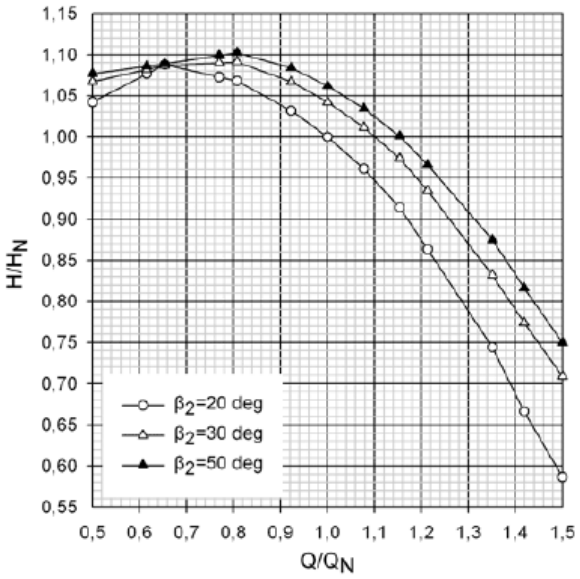

Fig.8: Predicted head curves for the examined pump impellers [2].

The next is agrees with the numerical prediction results of the curve H-Q for exist impellers. The nominal volumetric flow rate and total head pressure are predicted numerically by computational fluid dynamic for the $\beta_2 = 20$ deg as $Q_N = 58.5$ m^3/h, and $H_N = 8.93$ m Where, H_N is the nominal head pressure and Q_N is the nominal flow rate. The nominal operation parameters are defined when the hydraulic efficiency reaches the maximum value.

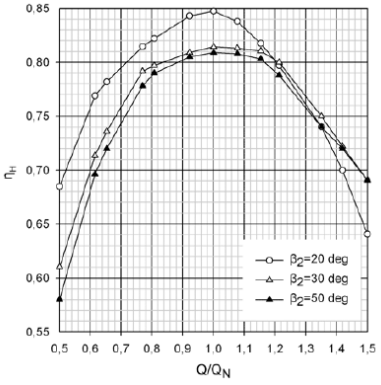

Fig.9: Predicted hydraulic efficiency [2].

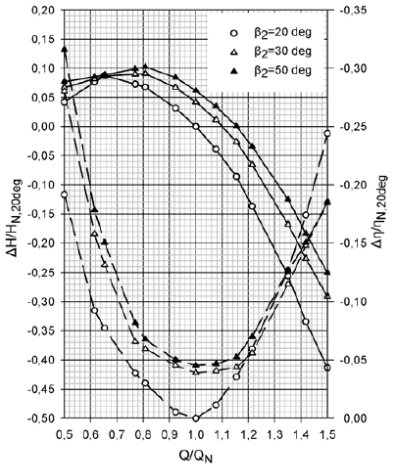

Fig.10: Percentage variation of the hydraulic efficiency [2]. (dash lines) and the head (solid lines) curves with outlet blade angle for the examined impellers.

The hydraulic efficiency differs with the operation conditions and against the non-dimension flow rate is illustrated in the Fig. 9. which shows that, at the optimal flow rate (nominal condition) the efficiency fluctuates form 0.81 to 0.845 for all impeller which are in reasonable agreement with the predicted value according to the applied design method. And it is clear the reduction of flow rate to 50% leads to 20, 25 and 28% drop in the hydraulic efficiency for β_2=20, 30 and 50 deg respectively. By similar approach, the increasing of flow rate with 50% leads to 25, 15 and 15% drop for the hydraulic efficiency too. The hydraulic efficiency curve for flow rate less than that nominal one decreases more rapidly with β_2=30 and 50 than for β_2=20 deg. In other case, when the flow rate is larger than the nominal, the opposite happens where, the curve of β_2=20 deg is steeper than the others. By comparison the three impellers at nominal operation conditions, the increasing of the outlet blade angle more than 30 deg reduces the hydraulic efficiency 3% almost.

The variation of the outlet blade angle causes a different performance curves for the three impeller, that can be expressed as a percentage variation with reference of the nominal head pressure values H/H_N and η_H at nominal capacity for outlet blade angle β_2=20 deg, as illustrated by Fig. 10. Thus, at the nominal condition, with increasing β_2 ten deg leads to 4.2% improvement for the head pressure and 3.9% reduction for hydraulic efficiency. If outlet blade angle increases 30 deg (20 to 50 deg), the head pressure will increase 6.2% and the hydraulic efficiency reduction is almost 4.5%.

1.3.2. Influence of the outlet blade angle on the static pressure [2]

Fig. 11 Shows that, the static pressure of the plane near the shroud for different outlet blade angle 20 and 50 deg. At the same radius position, the static pressure drops from the pressure side to the section side of the blade but this drop of the pressure decreases at the trailing edge of the blade. In addition, the patterns of the static pressure between the volute case and the impeller hub aren't the same. The difference is noticed by the pressure contour of the blade's surfaces at the pressure and section sides. This pressure variation doesn't make any additional losses in the pump which means that, each blade can gives a specific amount of energy to water lower than that described by Euler's equation. The static pressure differs with different outlet blade angle where, with increasing the outlet blade angle the static pressure becomes higher and higher.

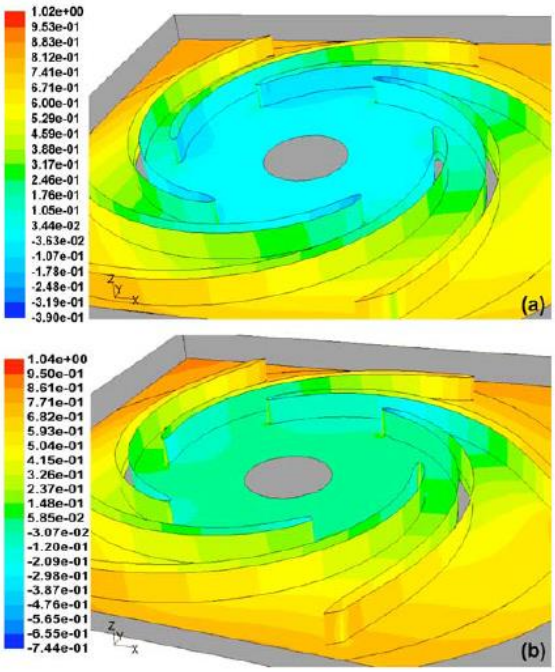

Fig.11: Static pressure (atm) at QN for the β2=20 deg (a) and β2=50 deg (b) impellers [2].

The lowest static pressure value inside the pump exists at the leading edge of the blade at suction side because of the interaction between the blade and the tongue. Moreover the other reason is because of the geometry and the design method of the blade.

1.3.3. Influence of the outlet blade angle on the velocities [2]

Similarly, the flow rate is usually dealt for greater or lower than the optimal operation condition, as well as for various outlet blade angle, Fig. 12 Shows the flow close to the tongue at optimal condition, the pattern confirms that, stagnation point position is located at the middle of the tongue edge. The angle β_2 influences on the changes of the relative velocity contours where, when the angle increases, circulation zone at the trailing edge of the blade established.

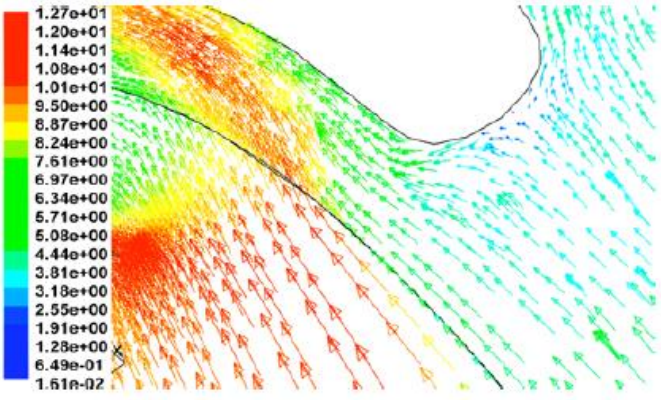

Fig.12: The absolute velocities (m/s) in the region of the tongue for the β2=20 deg impeller [2].

Usually, the absolute velocity contour is shown between the blades (blade passage) at off-design operation conditions. All rotors are working at nominal capacity range. When the impeller is operated at the nominal condition or more, the fluid forms a smooth flow through the blade

passage, except the flow around the end, where there is a region of the tongue. Due to the blade curvature and the flow direction appears a weak vortex at the pressure side of the blade, in the direction to leading edge which causes a low pressure in that region.

In contrast, if the impeller working at condition that is lower than the nominal one, the vortex are established at the leading edge of each blade. The velocity pattern doesn't suggest that, the velocity distribution is steady within the impeller zone.
In the region of the leading edge, non-uniform velocity distribution presents which is minimized in the outlet of the impeller. The difference velocity distribution at the leading edge of the blade (the entrance of the blade passage) because of the difference shape between the volute case and impeller, in addition inability of the fluid to fit the flow path.

1.4. Influence of the number of blade on the flow parameters in centrifugal pumps [5]

Chakraborty and K.M.Pandey [5] studied the effect of the number of blades in a centrifugal pump on the flow parameters (basically on static pressure and total pressure), and noted the changes of these parameters with variation of number of blades, 6 to 10 blades.

They checked the performance of the impeller with the same rotor diameter but with different number of blade for the centrifugal pump. The most influencing parameters on the centrifugal pump are outlet blade angle, number of blades of impeller and the outer diameter of impeller. The model was tested at speed 400 rpm and impeller's blade 4,5,6,7,8,9,10 and 12. In this study, the inner flow and centrifugal pump's characteristic was simulated and the results are predicted by Ansys Fluent software. Where the study was done based on the steady condition with moving reference frame to take the impeller motion interaction into account. For all impellers, the total pressure, efficiency, pump head and the static pressure were discussed. Where they noticed that, when the blades' number increases, the static pressure and the head increase too, but the performance of the pump which means the efficiency differs, in other words, it changes form minimum to maximum and to minimum again, that means there is an optimal number for the blades for each pump according to its optimal efficiency.

Andrzej [11], measured the parameters of a centrifugal pump at high speed working with open-flow impeller and radial blades. Where they noticed that, at high speed operation, the gained head pressure is large due to large outlet blade angle which gives the flowing flow at the out of the impeller high velocity and high dynamic pressure too. The kinetic energy converts to pressure in the volute case within the diffuser.

1.4.1. Mathematical formulations

Each mathematical model has a governing equations which represent this model in the software, this model is defined by combination of dependent and independent variables and other relative parameters for forming the differential equations of that model. The following equations are provided based on the computational model.

a- Navier-Stokes equations for steady state case in two dimension style and for incompressible flow with a constant viscosity are as follow:

$$\frac{\partial U}{\partial X} + \frac{\partial U}{\partial Y} = 0 \tag{9}$$

$$\frac{\partial (UU)}{\partial X} + \frac{\partial (VU)}{\partial Y} = -\frac{\partial p_n}{\partial X} + \frac{1}{Re}\left(\frac{\partial 2U}{\partial X^2} + \frac{\partial 2U}{\partial Y^2}\right) \tag{10}$$

$$\frac{\partial (UV)}{\partial X} + \frac{\partial (VV)}{\partial Y} = -\frac{\partial p_n}{\partial X} + \frac{1}{Re}\left(\frac{\partial 2V}{\partial X^2} + \frac{\partial 2V}{\partial Y^2}\right) \tag{11}$$

Where, equation. (9) is continuity equation, equation. (10) and (11) momentum equation in both axises X and Y respectively.

$$X = \frac{x}{D}, \quad Y = \frac{y}{D}, \quad p_n = \frac{p}{\rho\, u_\infty^2}, \quad U = \frac{u}{u_\infty}, \quad V = \frac{v}{u_\infty}, \quad Re = \frac{\rho u_\infty D}{\mu}$$

b- Standard k-ε model and its transport equations:

K-ε model is the most used turbulence model because is the simplest and it gives the nearest results to the real one. This model solves two separate transport equations to allow the turbulence kinetic energy and its dissipation rate to be independently determined.

$$\rho \frac{DK}{Dt} = \frac{\partial}{\partial x_i}\left[\left(\mu + \frac{\mu_t}{\partial_k}\right)\frac{\partial k}{\partial x_i}\right] + G_K + G_b - \rho\varepsilon - Y_M \tag{12}$$

$$\rho \frac{D\varepsilon}{Dt} = \frac{\partial}{\partial x_i}\left[\left(\mu + \frac{\mu_t}{\partial_\varepsilon}\right)\frac{\partial \varepsilon}{\partial x_i}\right] + C_{1\varepsilon}\frac{\varepsilon}{k}\left(G_K + C_{3\varepsilon} * G_b\right) - C_{2\varepsilon} * \rho * \frac{\varepsilon^2}{k} \tag{13}$$

Where the turbulent viscosity is: $\mu_t = \rho * C_\mu * \frac{k^2}{\varepsilon}$

G_b, generated turbulence kinetic energy because of the buoyancy, G_k, is the generated turbulence kinetic energy because the velocity gradients. All terms that include the turbulent kinetic energy K and the dissipation rate, are shared by the fluid.

1.4.2. Pump geometry

Table. 1: Pump geometry details

impeller						
Description	Blade number	Inlet blade angle	Outlet blade angle	Blade shape	Impeller inlet diameter	Impeller outlet diameter
value	4,5,6,7,8,9,10,12	25	33	Circular arc	80 mm	168 mm
volute						
Description	Inlet diameter	Volute tongue radius	type			
value	80 mm	52 mm	Semi-volute			

1.4.3. Numerical simulation and performance prediction

By Ansys Fluent, the model was simulated with steady condition, and K-ε model as the turbulence model with the pressure information at the inlet and the outlet, in addition with condition no slip velocity on wall surface. It is clear as illustrated in Fig. 13 that, the difference in static pressure within the pump model with different blades' number. The static pressure increases from the inlet to the outlet of the impeller, on the pressure side of the blade the static pressure is larger than the suction for the same impeller's diameter. The static pressure at the outlet of volute increases when the blades' number increase and the pressure distribution becomes worse, but at diffusion section become better.

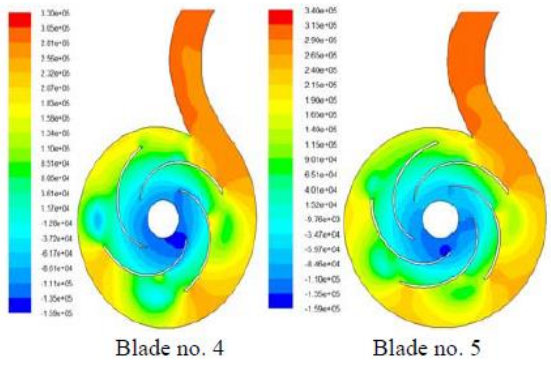

Fig.13. Static pressure (Pascal) distribution for different impeller [5].

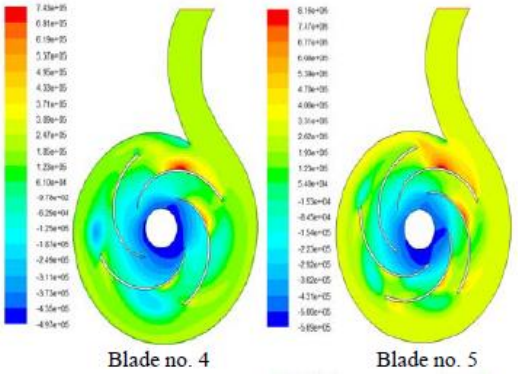

Fig.14. Total pressure (Pascal) distribution for different impellers [5].

Fig. 14 Shows the total pressure distribution of the centrifugal pump for same model but different blades' number. It illustrates that, increasing the blades' leads to increase total pressure too.

1.5. Prediction algorithm for Head and Efficiency pumps [5]

From basics of fluid, the head pressure and the total efficiency can be calculated by:

$$H = \frac{P_{out-P_{in}}}{\rho g} \tag{14}$$

$$\eta = \left(\frac{1}{\eta_v \eta_H} + \frac{\Delta p_d}{p_e} + 0.03\right)^{-1} \tag{15}$$

Where, P_{in} and P_{out} are total pressure at the inlet of the impeller and at the outlet of the volute, ρ is the density of the fluid, g is the acceleration of the gravity, ΔP_d is the disk friction losses, P_e is the hydraulic power of the water which is calculated by $P_e = \rho g h Q$, η_v and η_H are the volumetric and hydraulic efficiencies of the pump, η is the total efficiency.

Table. 2: Estimated value of efficiency and head pressure

parameter	Head [m]	Efficiency (%)
Blade no.4	29.01	73.55
Blade no.5	23.75	73.89
Blade no.6	32.98	73.63
Blade no.7	33.55	75.66
Blade no.8	34.46	74.16
Blade no.9	34.98	73.30
Blade no.10	37.76	78.16
Blade no.12	38.39	74.07

Based on the information from the table. (2) and Fig. 15 is clear that, when the blades' number increases, the head increases too in all cases, in contrast if the number is too high then, crowding phenomenon at the outlet will increase the velocity, that leads to more hydraulic losses, in other words the total efficiency will decrease. Also the interface between the fluid and blade wall will increase by increasing the blades' number which means more obstruction and more losses. In other hand, if the blades are few then the losses will appear due to diffuse extent of flow passage. From the Fig. 15 is clear that at 7 and 10 blades, the efficiency is maximum and at 12 blades is clearly there is efficiency drop which means bad design.

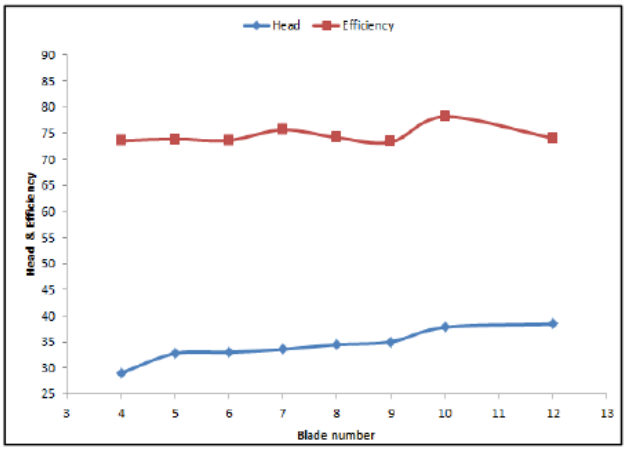

Fig.15: Head and efficiency for different blades' number [5].

1.6. The influence of speed on the performance of centrifugal pump [12]

The basics of turbo machinery say that, change of rotational speed for the impeller in centrifugal pump moves or shifts the performance curve of the pump characteristic upwards or downwards. In other words, the operation point can be in the sufficient zone or different zone according to the speed.

1.6.1. Simulation analysis

Huimin [12] and others Created the impeller by UG software and then they exported it to Ansys Fluent for doing simulation. The pump geometry and parameters are in table. (3) below.

Table. 3: Parameters of centrifugal pump

Flow	Head	Shaft power	Speed	Efficiency	Outlet diameter	Inlet diameter	Stage
20 [m^3/h]	3.8 [m]	2.61 [kW]	1450, 2900 rpm	64 %	50 mm	22 mm	I

In order to get the pump performance at different speed, **Huimin [12]** simulated above model with two speed 1450, 2900 rpm. The flow field in both cases is very close but the difference is the parameter values, and the flow stream is almost the same.

The static pressure has the lowest value at the inlet of the pump due to suction process, and then it gets more power by the impeller and by the diffuser in the volute area. In the volute, increasing the cross section area leads to increase the static pressure too, and finally at the outlet, the static pressure gets the maximum value.

1.6.2. Curve of performance

The performance curve and the efficiency can be calculated by previous equations (14) and (15), but for different parameters we can calculate the performance curve, required power and the efficiency by following equations:

$$H = \frac{P_{out-}\, p_{in}}{\rho g} + \frac{C_{out}^2 - C_{in}^2}{2g} + \Delta H \tag{16}$$

$$p_l = M.\omega \tag{17}$$

$$\eta = \frac{\rho g Q H}{P} \tag{18}$$

Where, C_{out} and C_{in} are the velocities at the inlet and the outlet, ΔH is the head different between the inlet and the outlet, M is the impeller torque, ω in angular velocity, P is the required power for pumping.

1.7. Shape effect of the volute tongue on performance of a centrifugal pump with very low specific speed [13]

In order to improve the pump efficiency and its characteristic and get the optimal design with perfect flow stream at low specific speed, **Nguyen and the others [13]** studied variation of shapes for volute tongue, by changing an angle that is able to modify the length of the tongue when it is larger, six angels were studied -5, 0, 5, 20, 35, 45 deg. They noticed the highest efficiency is at 5 degree compared with other angles.

It is clear based on Fig. 16 that, the highest efficiency of the pump is at 5 deg of changeable angle. At 0 deg, the performance starts dropping, and when the angle is more than 5 deg, the efficiency fluctuates slightly.

Regard to this study, the conventional design is bad choice for very low specific speed N_s, because the modification of the volute tongue causes an improvement for pump efficiency

between 72.7% to 75%. This achievement can happen just when the volute angle is five and the outlet blade angle is 34 deg.

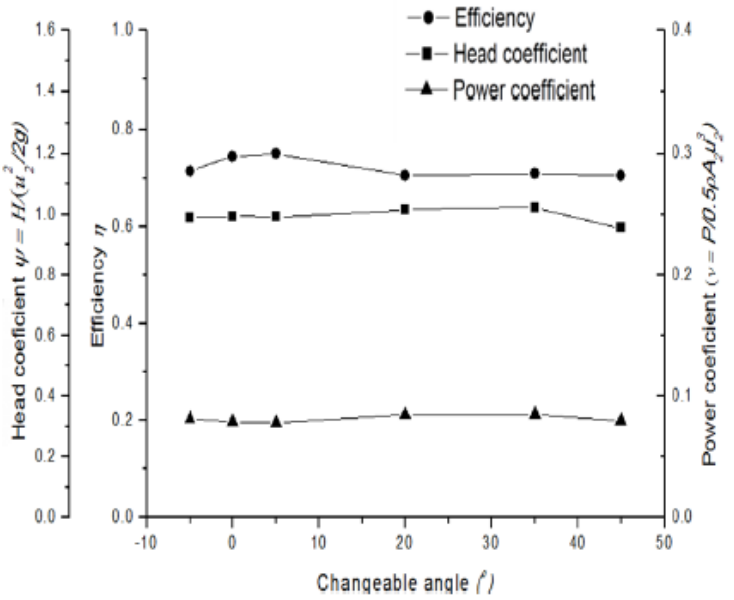

Fig.16: Effect of the changeable angle of the volute tongue [13].

1.8. Similarity and dimensionless characteristics of centrifugal pump

1.8.1. Dimensionless numbers

One of the most important method for investigation of complex fluid problems is dimensionless analysis. Recently, **Timár [9]** used this method for solving physical or technical problems. According to him, determination all important variable that related, connected and influence the problem solution, and arrange them in matrix which called dimensional matrix. This matrix divided into two sub-matrix residual and quadratic core matrixes, converting these two matrixes into unity by arithmetic operations, dimensionless numbers regarding to studied system were gotten. In the case of centrifugal pump, just one variable must be dependent and it is usually the specific energy gH or the pump efficiency. After that, all independent variable that influence the object variable should be in relevance list of variable. In case centrifugal pump, the independent variables are volumetric flow rate Q, rotational speed n, dynamic viscosity μ and fluid density ρ. In addition, the geometry quantities are taken in account too, like impeller's outer diameter D and the other length that are necessary for pump geometry. Mathematical functions between the dependent and independent variable are given by following equations:

$$F\ (gH, Q, D, n, \rho, \mu) = 0 \tag{19}$$

$$G\ (\eta, Q, D, n, \mu, \rho) = 0 \tag{20}$$

According to previous equations, we can write both dimensional matrixes, residuals and core one which expressed as (21). Where, l is the length, t is the time, m is the mass.

To get dimensionless numbers as mentioned previously, it is necessary to recalculate matrix (21) by linear operations, it was done by transform the core matrix to unity matrix.

	ρ	D	n	gH	Q	μ
m/kg	1	0	0	0	0	1
l/m	−3	1	0	2	3	−1
t/s	0	0	−1	−2	−1	−1
	core matrix			residual matrix		

(21)

According to matrix (22) as **Timár[9]** mentioned, dimensionless number can be gotten as follow:

	ρ	D	n	gH	Q	μ
m/kg	1	0	0	0	0	1
l/m	0	1	0	2	3	2
t/s	0	0	1	2	1	1
	core matrix			residual matrix		

(22)

$$\psi = \frac{gH}{n^2\, D^2} \tag{23}$$

$$\varphi = \frac{Q}{n\, D^3} \tag{24}$$

$$Re = \frac{\rho\, n\, D^2}{\mu} \tag{25}$$

where, equation. (23) and (24) represent pump head coefficient and flow rate coefficient respectively, equation. (25) is Reynolds number which represent fluid inertia force to viscosity force of same fluid. In addition, **Kuritza and others [8]** mentioned the power coefficient equation. (26) and relative roughness equation. (27) can be gotten by the same way too as follow:

$$\chi = \frac{P}{\rho\, n^3\, D^5} \tag{26}$$

$$\xi = \frac{\varepsilon}{D} \tag{27}$$

Kuritza and others [8], according to equation. (23), (24) and (26) could getting efficiency relation as below:

$$\eta = \frac{\psi\, \varphi}{\chi} \tag{28}$$

Based on these dimensionless parameters (numbers) it is easy to get the pump characteristic lines (H vs. Q) , (P vs. Q) , (η vs. Q). Another benefits can be obtained by dimensionless numbers which is the possibility to apply the similarity laws of hydraulic machines, like for example, evaluation the performance of the same machine at different speed or by different impeller diameter.

1.8.2. Specific rotation velocity and centrifugal pump performance

Specific speed velocity Ns: is a number that was obtained by similarity laws, it remains as a constant for all similar machine. This number is considered as the shape coefficient of the impeller. It is defined as the rotation speed of a pump which is similar to another pump that gives mass flow Q = 1 m^3/s for head H = 1 m.

$$N_s = \frac{N \,.\, Q_N^{1/2}}{H_N^{3/4}} \tag{29}$$

Where, N in the impeller speed, Q_N and H_N are the nominal operation conditions of the pump

Pump geometry can be classified by the specific speed value as the table. (4) shows.

Table. 4: Classification of pumps by specific rotation velocity, **Kuritza [8]**:

N_s (rpm)	pump's type
< 10	Positive displacement - gears, vane, pistons, etc.
$10 \div 40$	Radial Centrifugal
$35 \div 85$	Helical Centrifugal
$80 \div 150$	Diagonal Centrifugal
$125 \div 500$	Axial

Pumps' types depend on the specific speed and the flow rate as Fig. 17 clearly shows that, the tendency to increase the flow rate by increasing the specific speed.

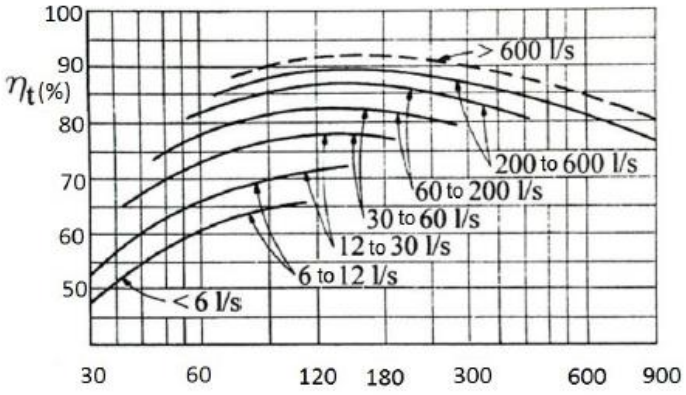

Fig.17: Efficiency regarding to the specific speed by range of discharge [8].

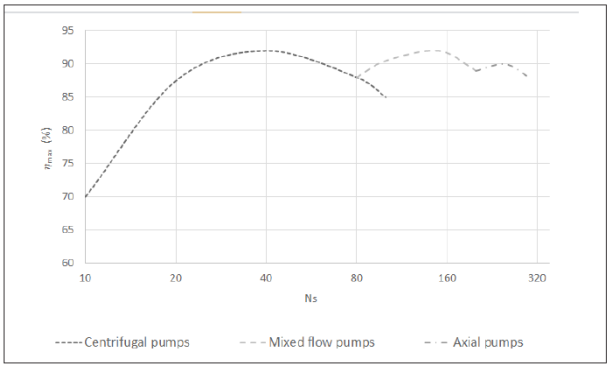

Fig.18: Efficiency of centrifugal, mixed and axial pump according to the specific speed [8].

1.9. Characteristics of centrifugal pumps [15]

1.9.1. Principle of energy conversion within a centrifugal pump

The fluid obtains his energy in the centrifugal pump by hydrodynamic means. Complex flow pattern in one dimension representation in the impeller allows the transferred energy to be computed by the fluid flow momentum theory (Euler equation).

$$T = \rho . Q_{out} . (c_{2u} . r_2 - c_{1u} . r_1) \quad (30)$$

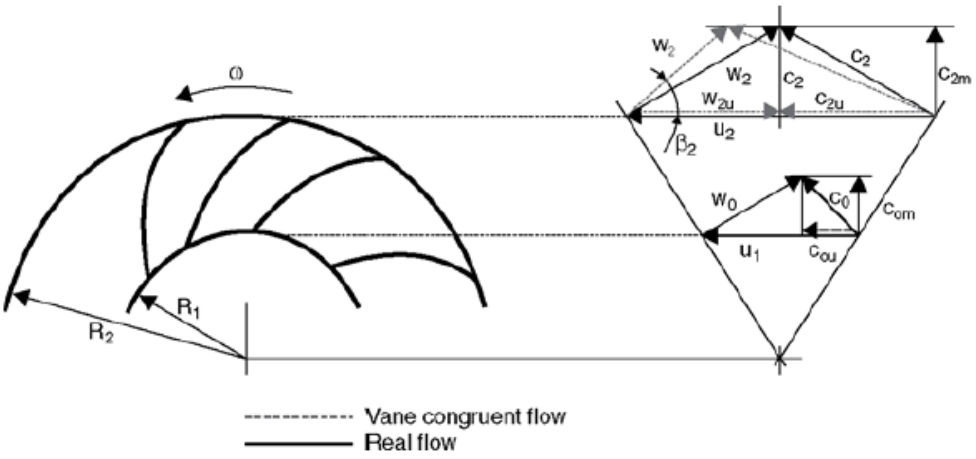

Fig.19: Velocity triangles diagram [15].

Where, T is the impeller torque, C_{2u} and C_{1u} are the absolute velocity projection on the impeller velocity U at the outlet and the inlet respectively. In order to calculate the power, it can be obtained with multiply the torque by angular velocity. Where, $U_2 = r_2 * \omega$ and , $U_1 = r_1 * \omega$ as equation. (31) shows below:

$$P_L = M * \omega = \rho . Q_{out} . (c_{2u} . u_2 - c_{1u} . u_1) \quad (31)$$

The transferred power to mass unit of the fluid is define as the specific work Y_L done by the impeller. This specific work can be derived based on the equation. (31) as follows:

$$Y_L = \frac{p_l}{\rho . Q_{out}} = (c_{2u} . u_2 - c_{1u} . u_1) \quad (32)$$

This provided power is less than the impeller power due to the friction and hydraulic losses, these losses are considered in the hydraulic efficiency as illustrated below:

$$Y = Y_L * \eta_H \quad (33)$$

The specific power depends only on the geometry of the pump and its components. In other words, the flow rate and the peripheral velocity are independent of the pumped fluid and of gravity too, that means the given power van be provided by any other pump in the same amount even to different fluid such as water, air or mercury. However, the deflection of flow characteristic of the impeller and the other losses must be known, theses data can be determined by such type of precision tests.

1.9.2. Power, losses and efficiency

The pump (impeller) flow Q usually consists three part mainly,

1) Leakage flow rate (due to the impeller sealing rings) Q_L.
2) Balancing flow rate Q_E.
3) Useful flow rate (the obtained one at the outlet) Q_{out}.

Based on these, equation. (29) will consider all leakage as follows:

$$P_L = T * \omega = \rho . (Q_{out} + Q_E + Q_L) . (c_{2u} . u_2 - c_{1u} . u_1) \quad (34)$$

These kinds of flow rate forms new efficiency which called volumetric efficiency η_v.

$$\eta_v = \frac{Q_{out}}{Q} = \frac{Q_{out}}{Q_{out} + Q_E + Q_L} \quad (35)$$

In ideal operation condition, P_L is the required power that is necessary to operate the pump, but in the real case extra power is required due to additional losses which must be taken into account. The required power for pump operation can be written in form as demonstrated below:

$$P = \frac{\rho . Q_{out} . (c_{2u} . u_2 - c_{1u} . u_1)}{\eta_v} + P_{losses} \quad (36)$$

Where, P_{losses} is the losses in pump, whether if it is frictional or mechanical losses. Pump efficiency is the term which defined as the ratio of useful hydraulic power divided by the supplied power to the pump shaft.

$$\eta = \frac{P_Q}{P} = \frac{\rho . Q_{out} . Y}{P} = \frac{\rho . Q_{out} . g . H}{P} \quad (37)$$

1.9.3. Behavior of Centrifugal Pumps in Operation

The term of pump characteristic curves indicates to the curve that explain the pump performance and how it develops during operation process. The head pressure , input power and the efficiency at constant impeller rotation are demonstrated in the Fig. 20, 22 and 23 against the flow rate.

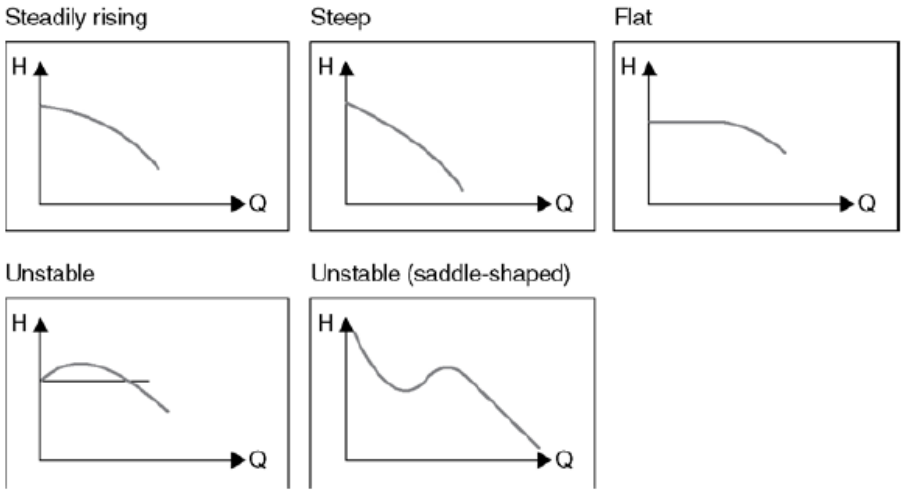

Fig.20: Typical curves of pump characteristics of centrifugal pump [15].

Fig. 20 Shows different shapes of pump characteristic based on the operation condition, the pump design and the condition of operation place. Where, at low specific speed the slope of head characteristic is small (flat curve) in contrast, at high specific speed, the head is very steeper.

Characteristic curve of a centrifugal pump is indicated as stable when the head declines steadily from the lowest flow rate to the maximum operation point in other words, when the slope of the curve is negative dH/dQ. In case of radial pumps, stable performance curve can be obtained by the following orders:

1- Small outlet blade angle.
2- Limited number of blades.
3- Relatively large outlet impeller width.

Unstable pump characteristic is shown in the Fig. 21 with interaction with the pipe layout curve, instability of the pump performance leads to oscillations and pipe vibration.

The head-flow rate curves for different impeller diameter and the constant efficiency lines are shown in the Fig. 22.

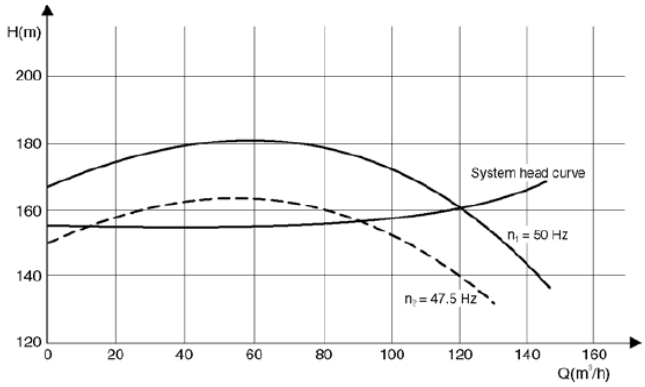

Fig.21: Unstable characteristic of a centrifugal pump with pipe layout curve interaction [15].

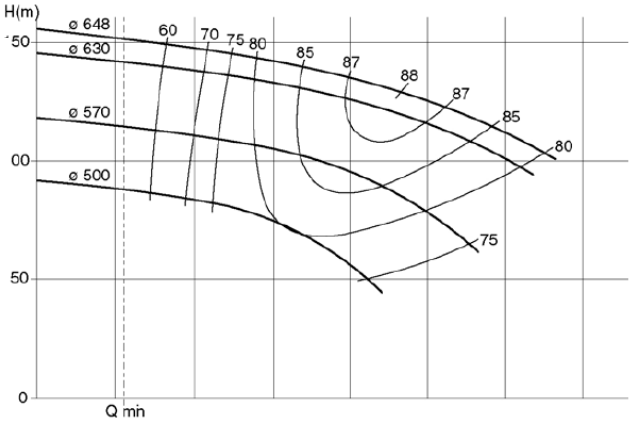

Fig.22: The pump characteristic and iso-efficiency at various impeller diameter [15].

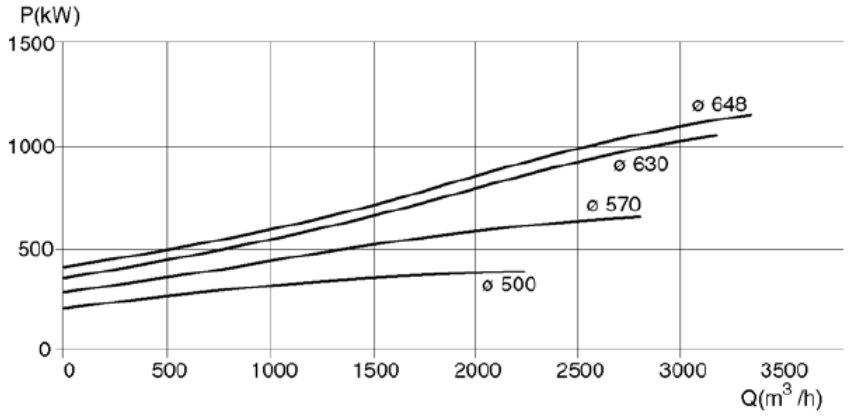

Fig.23:The pump capacity curve against the flow rate at various impeller diameter [15].

Fig.23 Shows the required power of pump operation for various impeller diameter, the consumed power increases with increasing diameter.

1.9.4. Control of centrifugal pump

To head pressure of the pump characteristic consists two main parts, first one is the static component H_{geo} which doesn't depend on the flow rate, the other one is the head losses H_{dyn} which increases with the increasing of flow rate due to the relation that configures the relation between the hydraulic losses and flow rate. The sum $H = H_{geo} + H_{dyn}$ is the required head to supply the required flow rate to the system. methods of pump output control:

1- Throttling: by controlling the throttle valve on the outlet of the pump which increase the resistant, that means the pump performance curve will intersect the pipe curve at lower flow rate and high head pressure.
2- Switching pump on or off.
   a) Operation in parallel: where some times the required flow rate is small, in this case we can turn some of the pumps off.
   b) Operation in series: same principle but for head pressure.
3- Speed control: as shown in Fig. 24 the pump characteristic varies with the impeller speed, thus the desired duty point can be achieved.
4- Bypass control: centrifugal pump usually controlled by the technic that called bypass (pipe line backs to suction side of the pump) in order to reduce flow rate or to help the pump to start in case unstable curve of the pump.
5- Impeller blade angle adjustment: especially for axial pump which can be provided by various outlet blade angle which gives facility to get various amount of flow rate
6- Cavitation control: it is used to reduce the flow rate due to the different specific volume between the water liquid and the water vapor, that can be achieved by various of available Net Positive Section Head $NPSH_a$.

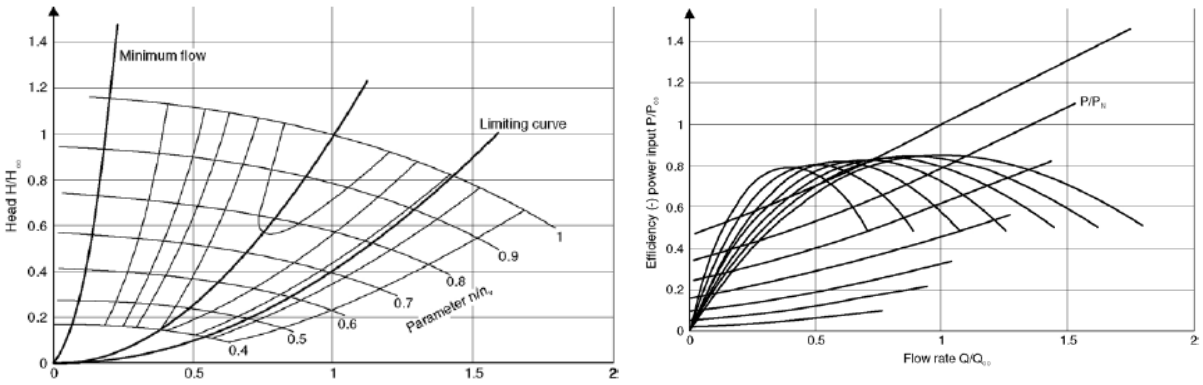

(a) (b)

Fig.24: The pump characteristic (a) and efficiency curve (b) at various impeller speed [15].

2. Experiment of a centrifugal pump with the aim of getting the characteristic curves

Centrifugal pumps are mainly used for transport of liquids. Knowing of characteristic curves of centrifugal pumps provides us with data about duty point and its efficiency, and can help us with selection of a best pump. Pump characteristics are usually plotted in graphical form and they are attached with curves of power (**P**) and efficiency (**η**) dependence on the flow rate of pumped fluid at various rotational speed (**N**). Behavior of these characteristics curves is not the same for all pump, it depends on different parameters not only on the pump geometry construction but on the boundary condition of the workshop place and the transported fluid properties too.

2.1. Firefighting unit's description

The experiment unit of firefighting H01 was assembled with a fuel engine, the frame was welded from the steel profiles and sheet metal parts. On the frame, there are stiffeners attached to the frame to minimize the vibration from the engine which is two-stroke gasoline engine, with maximum capacity 44 kW.

The engine is designed to be at its highest efficiency at 4500 rpm. The engine connected to the pump chamber by an aluminum frame, where the chamber is also seated on silent blocks. The torque transmission from the motor to pump impeller is secured by the shaft with the flexible coupling, the shaft is equipped with a double-row roller bearing.

Fig.25: Firefighting unit.

Sealing around the shaft, behind the pump chamber is ensured by a mechanical seal. The cooling water system is designed, so that water is sucked out of the chamber from the space below the impeller. The circuit is further guided so that, that heated water returns to the pump chamber at the suction point.

The pump suction side is connected to suction coupling, where the pump is fitted with two ball valves in addition with check valve too. Both valves have the same hose coupling. In addition the pump equipped with two pressure gauges, one of them for discharge side and the second one is for suction side. Other display and control elements included, such like control levers and choke control, start and stop buttons and speed counter. In addition, 12 V battery with current 28 Ah. For easier handling, the unit provided with four adjustable handles.

2.2. Experiment components

Pump experiment equipped with following components:

1- Water tank.
2- Three hoses: one for inlet and two for outlets.
3- Centrifugal pump which we want to test.
4- Two-strokes gasoline engine.
5- Flow meter.
6- Barometer.
7- Speed meter.
8- Ball valves.
9- Firefighting unit's frame.

Fig.26: Firefighting unit.

Fig.27: Water tank.

Fig.28: Flow meter.

Fig.29: Barometer.

2.3. Impeller geometry description:

Impeller geometry is demonstrated in Fig. 30, where the inlet and outlet diameters are 104.8, 174 mm, the width is 53 and 9.06 mm at the inlet and the outlet respectively. The impeller is provided by six backward blades with angles: $\beta_1 = 28$ deg and $\beta_2 = 32$ deg.

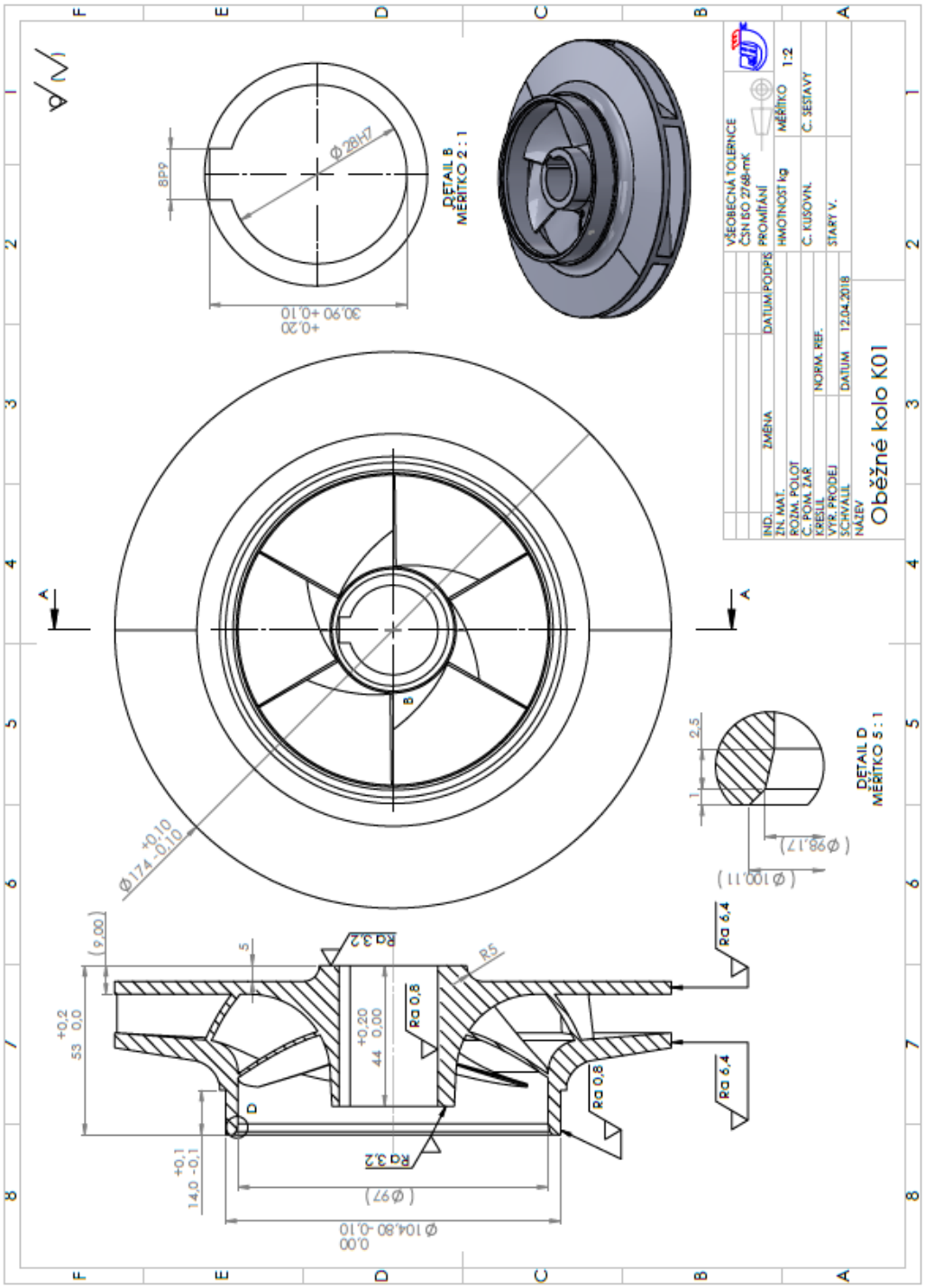

Fig.30: Impeller geometry, 2D drawing.

2.4. Experiment process:

An experiment data were measured at three impeller speed 4000, 3000 and 2000 rpm. Where the suction level of the pump was 40 cm above the water surface which exposed to atmospheric pressure.

Table. 5: Measured data of the firefighting pump at three speeds

N = 4000 rpm

Head [m]	**0**	**10**	**20**	**30**	**40**	**50**	**60**	**70**	**73**
Flow rate [l/min]	**1477**	**1450**	**1424**	**1385**	**1334**	**1248**	**1165**	**822**	**223**

N = 3000 rpm

Head [m]	**0**	**5**	**10**	**15**	**20**	**30**	**40**	**42**	
Flow rate [l/min]	**1382**	**1361**	**1346**	**1315**	**1288**	**1055**	**585**	**62**	

N = 2000 rpm

Head [m]	**0**	**5**	**10**	**15**	**20**				
Flow rate [l/min]	**1195**	**1018**	**931**	**713**	**264**				

According to measured data, the pump characteristic were plotted as Fig. 31 shows below, where the chart illustrate the effect of the impeller speed on the pump characteristic as **Kuritza [14]** explained this effect.

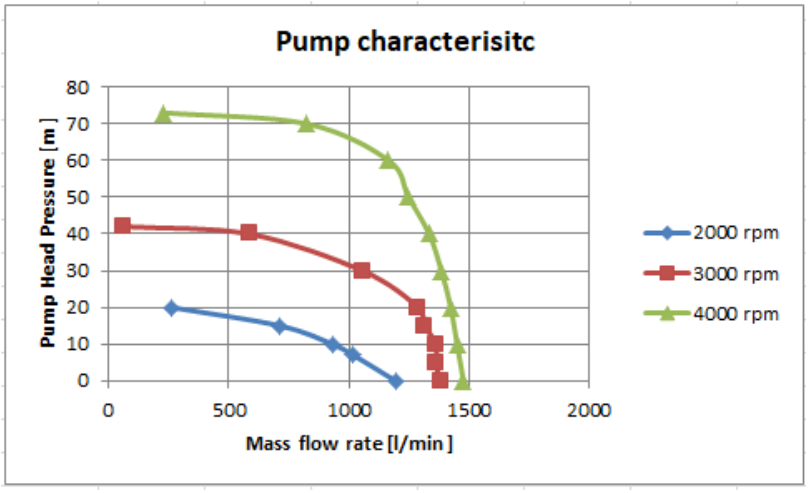

Fig.31: Measured pump's characteristic.

In addition, one more note Fig. 31 shows, the cavitation phenomenon happens clearly at high speed such as 4000 and 3000 rpm where their curves have a cut-off operation at high amount of flow rate. In contrast at low speed, for example; speed curve 2000 rpm is very smooth which means there is no cavitation as **Binama [16]** indicated in his paper

Fig. 32 shows the increasing of pump capacity at a constant NPSH curve and constant speed too. In addition the cavitation inceptions at a certain value of flow rate, where the head pressure curve deviates the optimal head curve and drops with straight line downward, that diagnoses the fault of the pump performance, and if the pump works continuously with increasing the capacity, the cavitation develops and leads to pump wall damage and other cavitation's effects.

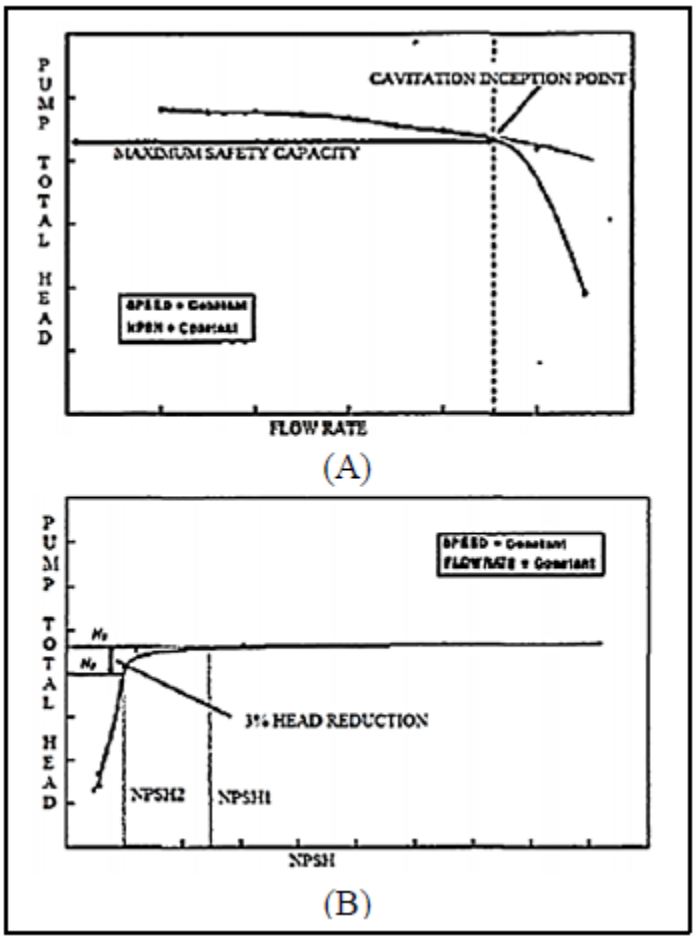

Fig.32: Cavitation effects on pump performance for both,
Head curve H-Q (A)
H-$NPSH_r$ curve (B).

3. Numerical simulation of firefighting pump model

In a wide range of applications centrifugal pumps are used, variation of fluid could be pumped by them at different low/high pressure. This study focuses on the pump characteristic and the possibility of cavitation happening at various impeller speed with variation of back pressure and for different NPSH.

3.1. Pump geometry

The firefighting centrifugal pump has one inlet with diameter 110 mm and double outlets with same diameter which is 75 mm as Fig. 33 shows. The geometry was drawn by ANSYS design modular software, the impeller diameter is 0.174 m supplied with six backwards blades with inlet and outlet blade angles $\beta_1 = 28$ deg and $\beta_2 = 32$ deg respectively, the outlet impeller width is 9.02 mm, the spiral volute has seven stationary blades too. The pump operated at different speed 4200, 3000 and 2000 rpm, the pump with inlet pressure -4000 Pa due to pump position in the experiment as mentioned above. Various of back pressure value was used in aim to get the mass flow rate of the pump at determined speed in order to obtain the pump characteristic at different speed.

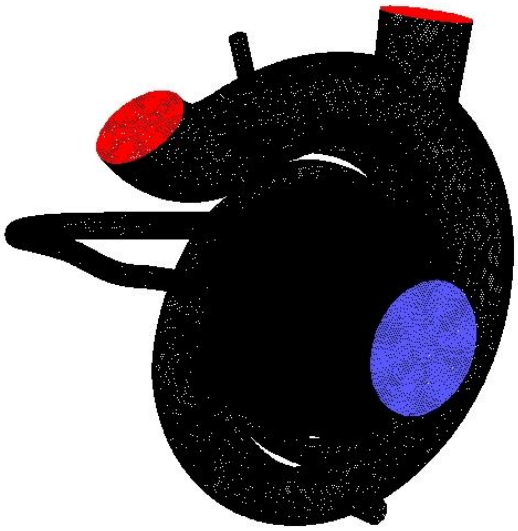

Fig.33: Pump model.

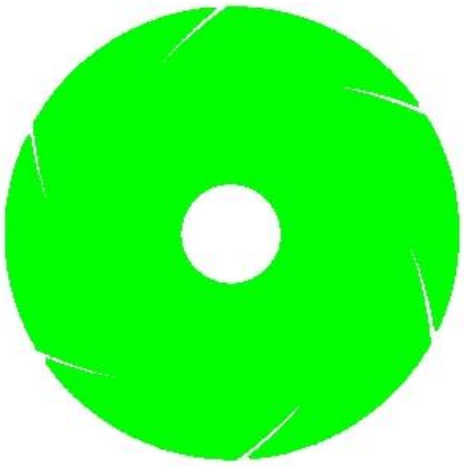

Fig.34: Impeller geometry.

3.2. Pump mesh

In this study, Fluent 18.1 was used to simulate how the fluid flows inside firefighting pump model, the space and fluid zones were divided into small control volume which called finite volume, almost 2.5 million hexahedral elements were generated for all model with different mesh density according to target area. For individual cell there are partial differential equations

which are transformed to algebraic equations and then they can be solved by some numerical techniques. And the required parameters are calculated for each cell too.

3.3. Numerical model

The numerical simulation was done by computational fluid dynamic method CFD by ANSYS Fluent software using a finite element based finite volume method to solve three dimensional equations such as Navier-stocks and continuity equation which are equations. (8), (9) and (10).

Pressure based type of solver was selected with steady case. Pressure based approach is used for different condition but it is usually used for incompressible fluid for various values of speed, the velocity field is obtained from the momentum equations, and the density is obtained from the state equation , in addition the pressure field is also obtained by manipulating continuity and momentum equations.

SST model under k-omega model is chosen as a turbulence model, this model is two-equation (eddy-viscosity) model. Using k-omega formulas in the inner part of the boundary layer makes the model directly useable all the way down to the wall through the viscous sub-layer, thus the SST K-omega model can be used without any extra damping functions. In addition, SST model can also switches to K-ε behavior in the free stream, thereby we could avoid the common problems that happen with K-omega at the inlet free-stream turbulence properties. SST k-omega model has a good behavior in adverse pressure gradients and separation flow. SST k-omega model generates too large turbulence level in regions with large normal pressure, such as stagnation regions. The SST model is recommended for high accuracy boundary layer simulations. No other model was used for getting pump characteristic, with neglect the cavitation phenomenon firstly and no heat transfer and no phase change. Water liquid was added to the solver to consider it as a working fluid in the fluid zones.

3.4. Boundary conditions

Boundary conditions are constraints necessary for the solution of a boundary value problem. A boundary value problem is a differential equation to be solved in a domain on whose boundary a set of conditions is known. It is opposed to the “initial value problem”, in which only the conditions on one extreme of the interval are known. Boundary value problems are extremely important as they model a vast amount of phenomena and applications, from solid mechanics to heat transfer, from fluid mechanics to acoustic diffusion.

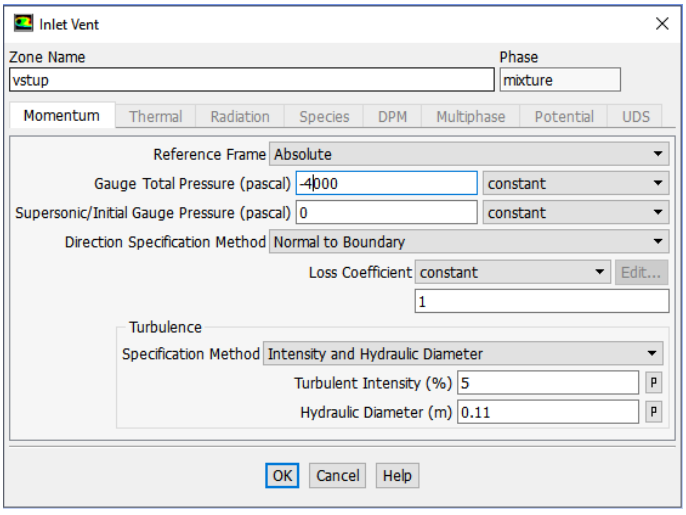

Fig.35: Inlet boundary condition window.

They rise naturally in every problem based on a differential equation to be solved in space, while initial value problems usually refer to problems to be solved in time. Pressure data are known at vents, where the pressure at the outlet set as -4000 Pa as a total gauge pressure with 5% turbulent intensity, and at the outlets the back pressure was changed many times according to the required following steps of simulation. The impeller zone is defined as a rotating zone with different rotation speed as mentioned previously.

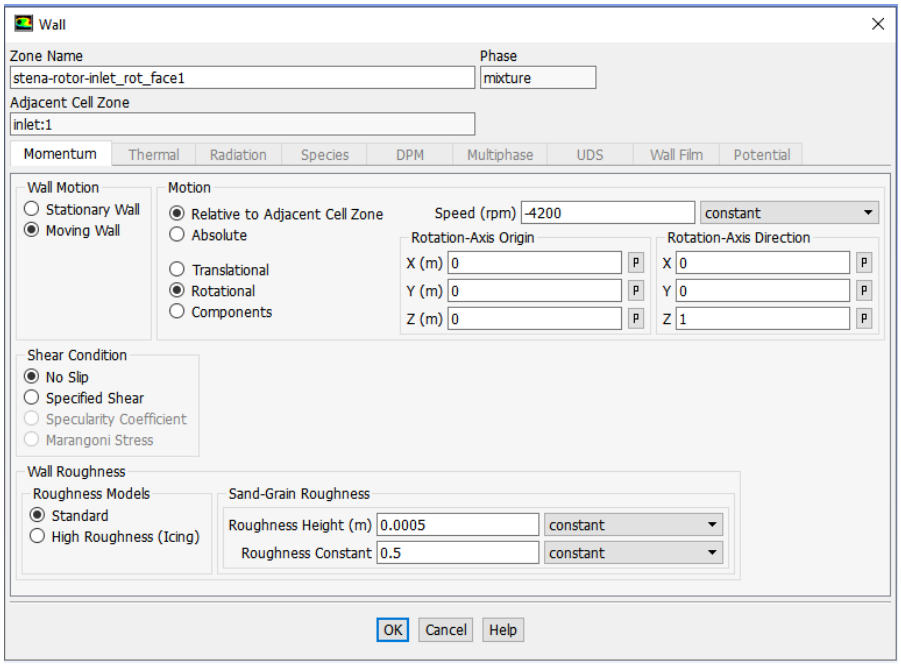

Fig.36: Rotor's boundary condition.

3.5. Simulation results and discussion

3.5.1. Pump characteristic

Knowledge about the centrifugal pump performance usually is known by drawing pump characteristic and see how the flow develops within the pump machine and detect the weak areas in it. Static pressure contour can give a primary idea about the pressure distribution at different positions of the pump, that means a possibility knowledge of cavitation. in addition, the velocity vectors can illustrate the flow directions and its values at various positions and predict the average value of this velocity on any target surface that we want to know the velocity average on it.

The simulation processes gave a group of results, by this numerical results, the pump characteristic was created. Table. (6) Shows the simulation results for different impeller speed as follows.

Table. 6: Simulation results

Impeller speed = 4200 rpm				
Back pressure [bar]	**Mass flow rate [kg/s]**	**Inlet velocity [m/s]**	**Outlet velocity [m/s]**	**Inlet static pressure [kPa]**

0	52.520	7.587	9.29	-61.48
1.5	46.0142	6.64	8.82	-48.05
3	40.316	5.83	8.24	-37.97
4.5	34.4429	4.97	6.93	-28.66
5	32.7063	4.72	6.25	-26.29
5.5	30.2932	4.37	5.67	-23.14
6	27.2265	3.93	5.23	-19.48
6.5	23.1022	3.33	4.20	-15.13
7	17.5953	2.53	3.58	-10.46
7.4	9.7003	1.85	2.61	-7.53
7.4	0			
Impeller speed = 3000 rpm				
Back pressure [bar]	**Mass flow rate [kg/s]**	**Inlet velocity [m/s]**	**Outlet velocity [m/s]**	**Inlet static pressure [kPa]**
0	35.889	35.90	7.03	-30.90
1	31.853	31.85	6.56	-25.15
2	25.946	29.95	4.97	-18.10
3	19.736	19.73	3.58	-12.14
3.3	16.496	16.49	3.05	-9.67
3.5	13.659	13.65	2.51	-7.87
3.7	0			
Impeller speed = 2000 rpm				
Back pressure [bar]	**Mass flow rate [kg/s]**	**Inlet velocity [m/s]**	**Outlet velocity [m/s]**	**Inlet static pressure [kPa]**
0	23.850	3.44	4.46	-15.86
0.5	20.368	2.94	3.83	-12.65
1	16.170	2.33	2.94	-9.45
1.25	13.579	1.95	2.5	-7.83
1.4	11.579	1.67	2.07	-6.80
1.6	0			

Pump characteristic curves for different speed are configured by Fig. 37. which shows how the pump characteristic curve differs with changing the impeller speed where, with increasing the impeller speed, the flow rate and back pressure increase too.

At speed 4200 rpm, the maximum head pressure is almost 7.4 bar with maximum mass flow rate 52 kg/s, at another speed such as 3000, 2000 rpm the maximum back pressure is 3.7 and 1.6 bar

respectively, the same for the flow rate where, the maximum flow rate for speed 3000 and 2000 rpm 36 and 23 kg/s respectively. These results are identical with the previous studies which were mentioned above **[15]**.

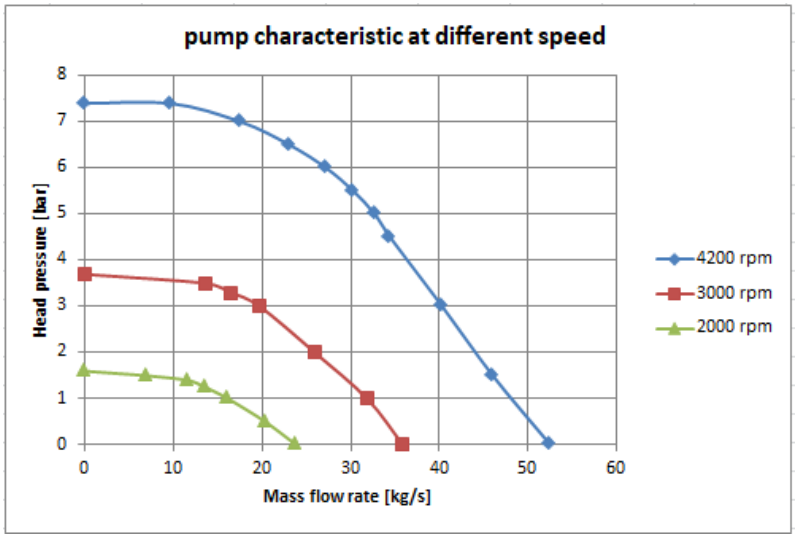

Fig.37: Pump characteristic for three different speed.

Maximum pressure that we can get by the pump is the dynamic pressure, it depends on the impeller speed and diameter, dynamic pressure can be calculated by following formula:

$$P_{dyn} = \rho * \frac{U^2}{2} \tag{38}$$

According to equation. (38) the maximum pressure we can get by this pump is 7.32, 3.73 and 1.66 bar at three speeds 4200, 3000 and 2000 rpm respectively.

For more understanding of pump performance and its efficiency, the hydraulic power of the water was calculated and compered with the consumed power by the pump's rotor and thus, pump efficiency can be obtained based on equation. (37).

3.5.2. Required power for the pump and its total efficiency

Table. 7: Power data and efficiency

Impeller speed = 4200 rpm				
Back pressure [bar]	**Moment [N.m]**	**Consumed power [kW]**	**Hydraulic power [kW]**	**Efficiency [%]**
0	80.1576	35.255	0	0
1.5	74.6725	32.842	6.902	21.01
3	69.1935	30.432	12.094	39.74
4.5	66.2673	29.145	15.499	53.17

5	65.6154	28.859	16.353	56.66
5.5	63.6587	27.998	16.661	59.50
6	60.4764	26.598	16.335	61.41
6.5	57.2045	25.159	15.016	59.68
7	51.5866	22.688	12.316	54.28
7.4	49.1810	21.630	7.178	33.18
7.4				0
Impeller speed = 3000 rpm				
Back pressure [bar]	**Moment [N.m]**	**Consumed power [kW]**	**Hydraulic power [kW]**	**Efficiency [%]**
0	38.2717	12.023	0	0
1	37.4247	11.757	3.185	27.09
2	34.3184	10.781	5.189	48.13
3	31.1250	9.778	5.920	60.55
3.3	29.1713	9.164	5.443	59.40
3.5	29.1713	8.513	4.780	56.15
3.7	27.0989			0
Impeller speed = 2000 rpm				
Back pressure [bar]	**Moment [N.m]**	**Consumed power [kW]**	**Hydraulic power [kW]**	**Efficiency [%]**
0	17.821	3.732	0	0
0.5	16.525	3.460	1.018	29.42
1	14.780	3.114	1.617	51.92
1.25	14.111	2.955	1.697	57.43
1.4	13.205	2.765	1.622	58.66
1.5				51.682
1.6				0

Hydraulic power was calculated based on the back pressure and the flow rate at the discharge of the pump.

$$P_{hyd} = \rho \,.\, g \,.\, Q_{out} \,.\, H \tag{39}$$

According to table. (7), the pump efficiencies are illustrated in following figures against the flow rate and compared with the pump characteristic individually for each speed**.** Fig. 38:(a) shows the pump efficiency compared with the pump characteristic against the flow rate at 4200 rpm speed of impeller, where we could note the maximum efficiency for this speed is 61.5% at 7 bar

back pressure which gives almost 27.5 kg/s. Fig. 38:(b) demonstrates compared efficiency with the pump characteristic too against the flow rate but at impeller speed 3000 rpm, where we can see the maximum efficiency value is 60.5% at 3 bar back pressure and almost 20 kg/s. Same parameters realized in Fig. 38:(c) but for impeller speed 2000 rpm, the maximum efficiency is 58.66% at 1.4 back pressure for 11.5 kg/s as flow rate.

(a)

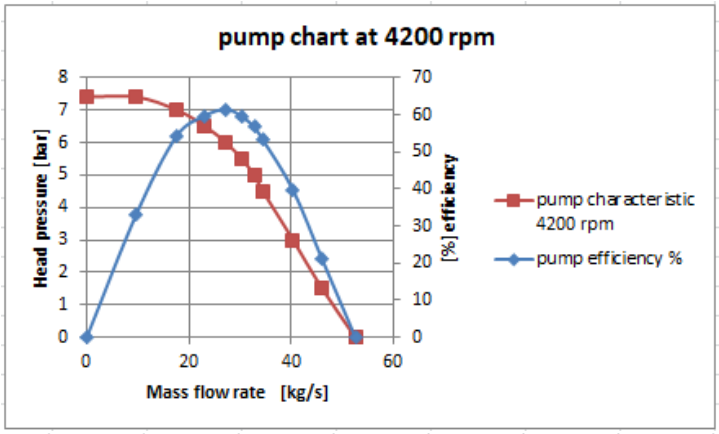

(b)

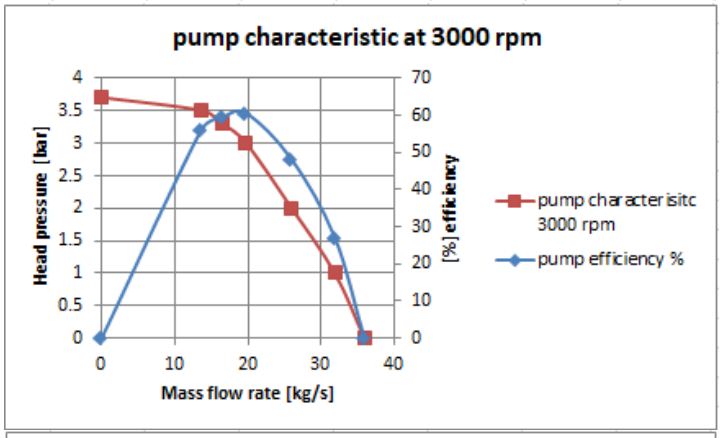

(c)

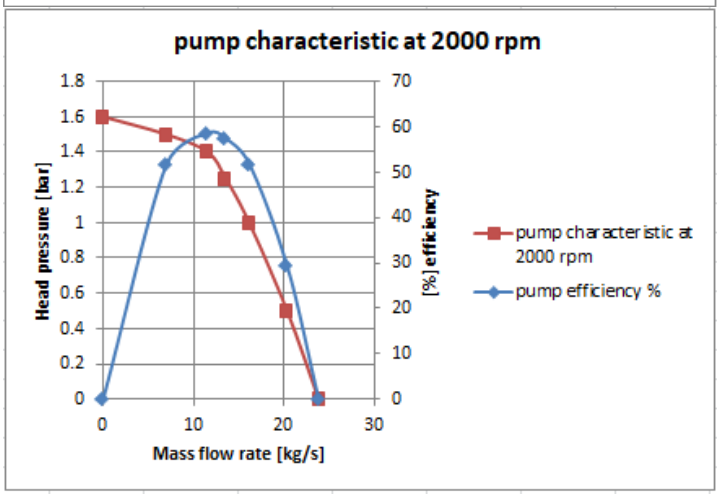

Fig.38: Pump's efficiency for different impeller speed.

3.5.3. Required power for pump operation

Required power for pump operation includes all power types (hydraulic, friction losses, local losses, mechanical losses and all other losses). Power vs. flow rate chart can be illustrated based on table. (6) and (7) where increasing in the required power exists with increasing of speed, that is clear in Fig. 39 where the maximum power when is at the highest speed which is 4200 rpm and then it decreases with decreasing impeller speed. From other view and based on the flow rate view, the required power is also increasing with increasing of flow rate, the main reason for that increasing is because of raise in velocity, that leads to more hydraulic losses in the fluid and requires more energy.

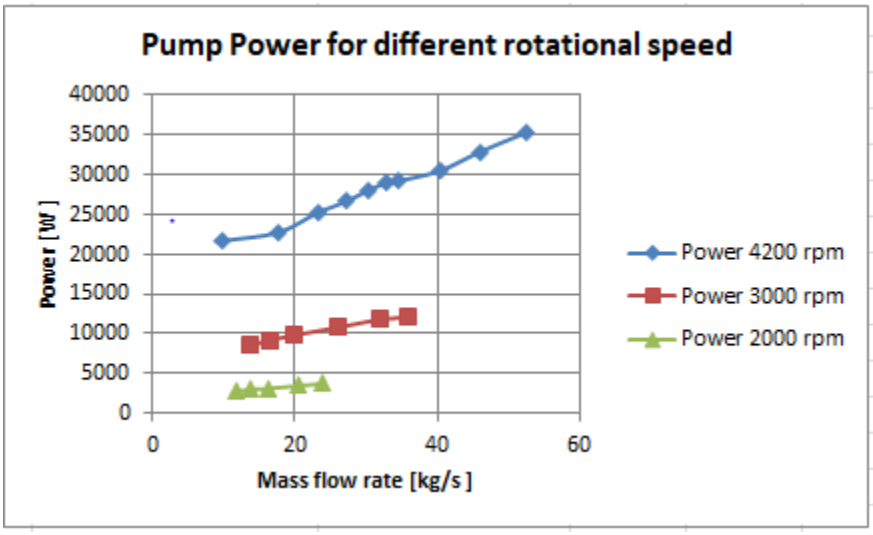

Fig.39: Required power for pump operation at different speed

3.5.4. Flow parameters contours

3.5.4.1. Static pressure contours at zero back pressure

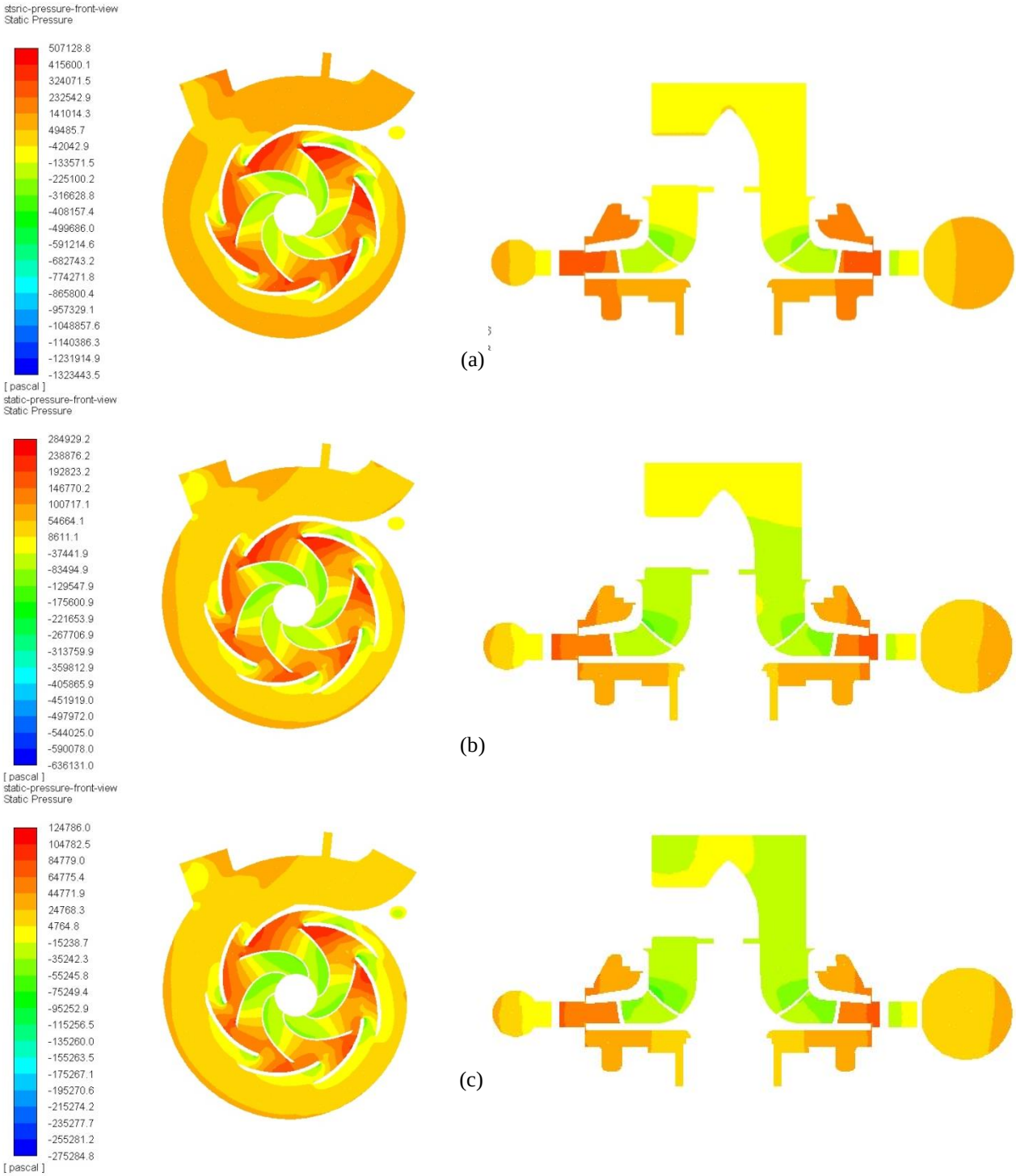

Fig.40: Static pressure for front and top views at three impeller's speed, 4200 rpm (a), 3000 rpm (b) and 2000 rpm (c) when the back prssure is zero.

3.5.4.2. Velocity contours at zero back pressure

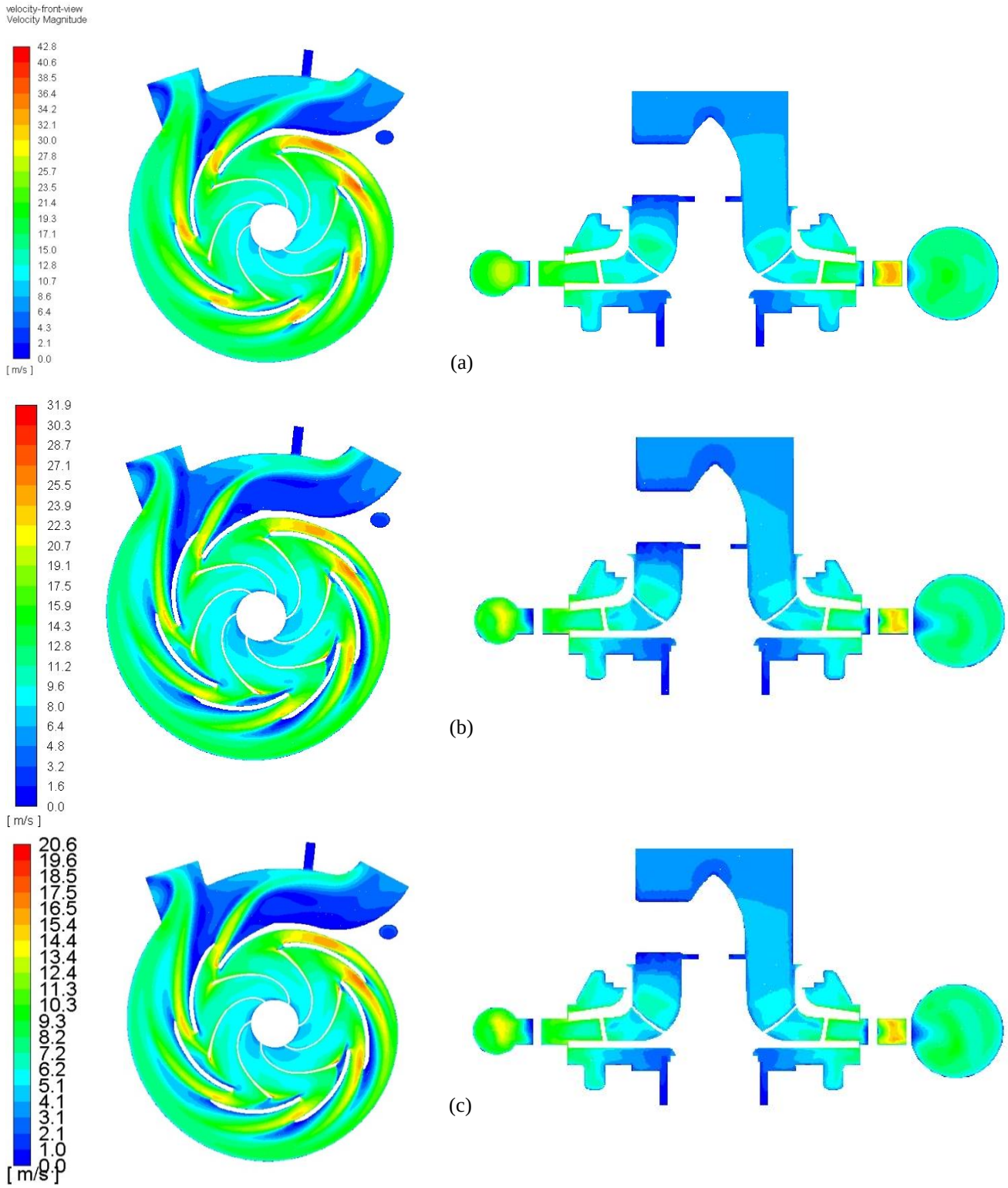

Fig.41: Velocity contours for front and top views at three impeller's speed, 4200 rpm (a), 3000 rpm (b) and 2000 rpm (c) when the back prssure is zero.

The impeller pump was operated with three different speeds to investigate and calculate the flow parameters such as velocity field and pressure field. Fig. 40 illustrates the static pressure field within the centrifugal pump for different impeller speed at the same back pressure which is zero bar. The static pressure has the maximum value at the highest speed 4200 rpm and it decreases with deceasing the impeller speed as configured above. In addition, we can note from Fig. 40 the maximum static pressure zones are placed on the pressure side of the blade and mainly at trailing edge of the blade. Likewise, Fig. 41 shows the velocity field within the same pump geometry and with same speeds where, we can note the maximum flow velocity at the outlet of the impeller due to the highest diameter at this position. the maximum velocity value we could obtain it by highest impeller speed and then it decreases with decreasing the speed.

3.6. Dimensionless characteristic of the simulated pump model

The fluid machinery is similar in three spheres: geometric, kinematic and dynamic. The geometrical similarity implies in the proportionality of the linear dimensions, the kinematic similarity implies that the vectors of velocity and acceleration, for corresponding points, are parallel and have a constant relation of their modules and, finally, the dynamic similarity is obtained when the identical types of forces acting on the system. To ensure that similarity criteria are met, a dimensional analysis must be performed.

In order to get the dimensionless curve of the pump for studied model which we simulated, and according to dimensions of that model and rotational speed the following information were obtained:

Speed of impeller = 3000 rpm
Diameter of the impeller D = 0.174 m

$$U = \frac{\pi \,.\, D \,.\, N}{60} = 27.33 \;\; m/s$$

water density $\rho = 1000$ kg / m^3
impeller outlet width $b_2 = 9.06$ mm
Based on the previous parameters, nominal characteristic head pressure and flow rate can be obtained as below:

$$P_{dynamic} = \rho * \frac{U^2}{2} = 1000 * \frac{27.33^2}{2} = 373464.5\ Pa$$

$$Q_{nominal} = \pi * D * b_2 * u = \pi * 0.174 * 0.00906 * 27.33 = 0.13535\ m^3/s$$

According to above equations, dimensionless characteristic can be calculated by equations. (40) and (41) as follow below:

Dimensionless pressure at outlet of the pump:

$$\Psi = \frac{P_{real}}{P_{dynamic}} \qquad (40)$$

Dimensionless flow rate at outlet of the pump:

$$\Omega = \frac{Q_{real}}{Q_{nominal}} \tag{41}$$

Same procedure is used for making dimensionless characteristic for 4200 rpm and 2000 rpm as below:

N = 4200 rpm:

$U = 38.26$ m/s , $P_{dyn} = 7.31913$ bar , $Q_{nominal} = 0.189$ m^3/s

N = 2000 rpm:

$U = 18.22$ m/s , $P_{dyn} = 1.65984$ bar , $Q_{nominal} = 0.090$ m^3/s

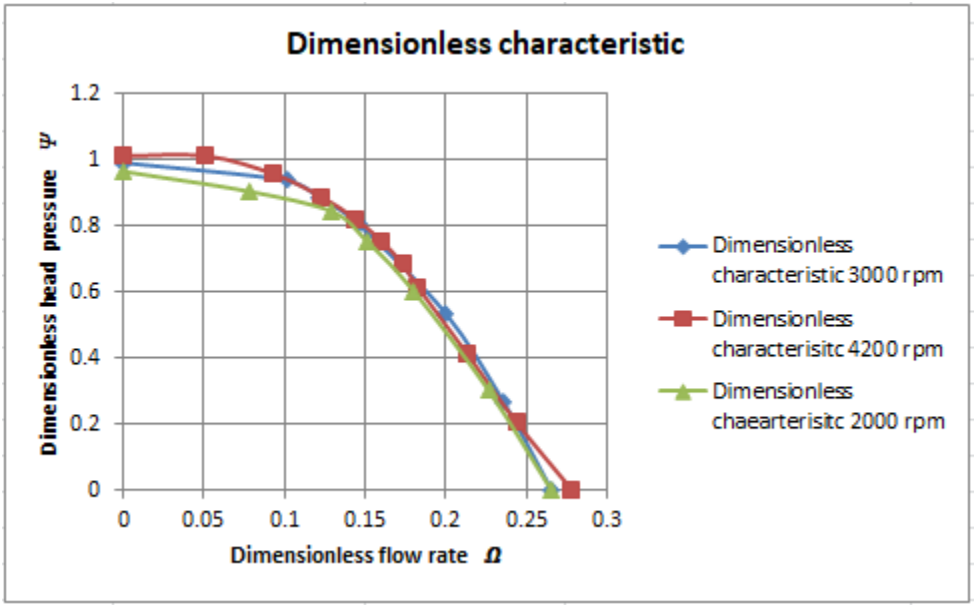

Fig.42: Dimensionless pump's characteristics (Ψ vs Ω).

Fig. 42 Illustrates the basic characteristic of the centrifugal pump in non-dimensional coordinates, where non-dimensional head is connected with non-dimensional flow rate. We can see in this coordinate, the dimensionless characteristic based on the equation. (40) and (41), almost one curve exist for all tested rotational impeller speed (N). variation on the impeller speed causes changes in the value of the Reynolds number, but these changes don't affect the dimensionless characteristic as illustrated in Fig. 42. In case of an estimation for the pump characteristic, but for different liquid, the same procedure can be used with different fluid parameters such as density, viscosity.

4. Cavitation investigation in the firefighting centrifugal pump

4.1. Cavitation definition

Cavitation is defined as bubbles formation process in the liquid when the fluid pressure decreases till it reaches the saturation pressure at constant ambient temperature. Fig. 43 Shows the thermodynamic diagram of Phase change, there are two main phase change processes, first one is boiling when the temperature reaches the saturation pressure at the atmospheric pressure, the second one is cavitation process which occurs as mentioned above.

Cavitation in a centrifugal pump has a significant effect on pump performance. Cavitation degrades the performance of a pump, resulting in a fluctuating in flow rate and discharge pressure. Cavitation can be also destructive to pump internal components. When a pump cavitates, vapor bubbles form in a low pressure region directly behind the rotating impeller vanes. These vapor bubbles move toward the oncoming impeller vane, where they collapse and cause a physical shock to the leading edge of the impeller vane. This shock creates small pits on the leading edge of the impeller vane. Each individual pit is microscopic in size, but the cumulative effects of millions of these pits formed over a period of hours or days can literately destroy the pump components.

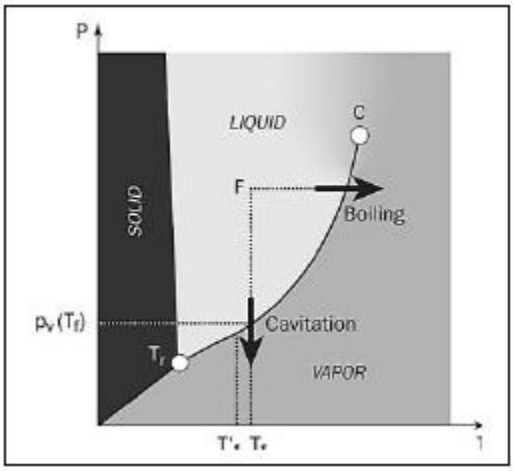

Fig.43 phase change mechanism [15].

Cavitation can also cause excessive pump vibration, which could damage pump bearings, wearing rings and more.

A small number of centrifugal pumps are designed to operate under conditions where there is a cavitation. These pumps must be designed and maintained to withstand the small amount of cavitation that occurs during their operations. Most centrifugal pump are not designed to withstand sustained cavitation. Noise is one indication that a centrifugal pump is cavitating. A cavitating pump can sound like a can of marbles being shaken. Other indications that can be observed from a remote operating station are fluctuating discharge pressure, flow rate and pump motor current.

4.2. Net positive suction head effect on the performance of the pump

Net positive suction head is the term that is usually used to describe the absolute pressure of a fluid at the inlet to a pump minus the vapor pressure of the liquid. The resultant value is known as the Net Positive Suction Head available. The term is normally shortened to the acronym NPSHa, the ‘a’ denotes ‘available’. A similar term is used by pump manufactures to describe the energy losses that occur within many pumps as the fluid volume is allowed to expand within the pump body. This energy loss is expressed as a head of fluid and is described as NPSHr (Net

Positive Suction Head requirement) the 'r' suffix is used to denote the value is a requirement. Different pumps will have different NPSH requirements depend on the impellor design, impellor diameter, inlet type, flow rate, pump speed and other factors. A pump performance curve will usually include a NPSH requirement graph expressed in meter or feet head so that the NPSHr for the operating condition can be established.

4.2.1. Pressure at the pump inlet [16]

The fluid pressure at a pump inlet will be determined by the pressure on the fluid surface, the frictional losses in the suction pipework and any rises or falls within the suction pipework system.

$NPSH_a$ = absolute pressure (at the water surface of lower reservoir) – vapor pressure – losses, piping and other fitting + static head

$$NPSH_a = \frac{1}{g}\left(\frac{P_a}{\rho} - \frac{P_v}{\rho} - h_{fs}\right) \pm Z_a \qquad (42)$$

Static head could be positive or negative according to the pump position for the lower reservoir where:

1- If the pump above the reservoir the static head will be negative, (suction lift).
2- If the pump below the reservoir the static head will be positive, (suction head).

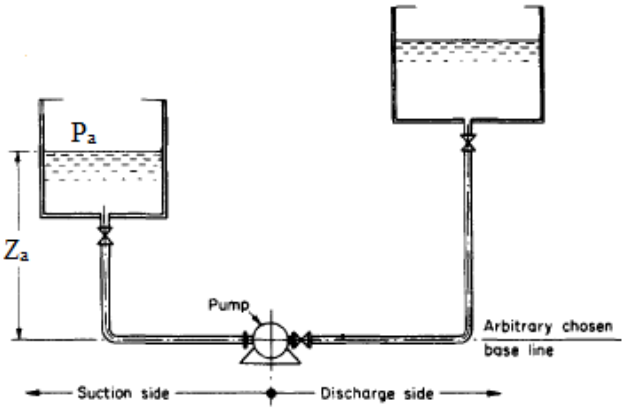

Fig.44: Pump position for the lower reservoir [16].

$NPSH_r$: is defined as the required net positive suction head for the pump to prevent cavitation, this value is set by the manufacturer because it depends on the pump geometry as mentioned above. The cavitation occurs when the available net positive suction head is lower than the required one as Fig. 45 Shows. The maximum flow rate that we can get without any bubbles exists when the required NPSH equals to available NPSH, before this point the cavitation won't happen, in contrast after this point, cavitation occurs.

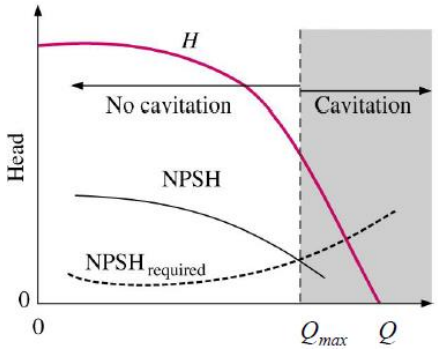

Fig.45 Interaction between $NPSH_a$ and $NPSH_r$ [16].

4.2.2. Increasing the NPSH available

Many systems suffer from initial poor design considerations. To increase the NPSHa consider the following:

a- Increase the suction pipe work size to give a fluid velocity of about 1 m/sec.
b- Redesign the suction pipework to eliminate bends, valves and fittings where possible.
c- Reset the height of the water reservoir.
d- Pressurized the fluid reservoir, but ensure that the pressure in the reservoir is maintained as the fluid level is lowered.

4.3. Cavitation detection methods

A- By measuring consumed electric data [16]

One of cavitation detection methods is the measuring the used current and voltage data that are required for pump operation process, this measuring data can be obtained by Voltage and current sensors. By the measured data, the power signal of the pump can be generated and spectrally analyzed to give a primary idea about the cavitation in the pump, and then undesired operation condition can be avoided to prevent bubbles formation on the impeller blade wall, or if the cavitation is already exist then, we can do a maintenance and some modification for operation conditions.

B- By monitoring of steady-state flow behavior [17]

Other effective method for detection cavitation is by behavior of the fluid within the system generally and within the pump especially. When there is cavitation that means the pressure is reduced to specific limit in the suction pipe therefore, the pump spaces don't fill completely because of the air bubbles, when we have a smaller amount of flow rate that means we have cavitation.

C- By high-speed monitoring of pressure and vibrations [17]

Cavitation phenomenon can be detected by measuring and monitoring the vibration of the components of the pump. Cavity inception can be seen for first time at very high frequencies, due to that reason, shock waves can be recorded in the area of cavitation. This shock waves can propagate and continue from its position to the pump component and the make a vibration, by measuring speed spectrum or acceleration spectrum of vibration we can determine if there is any cavitation or note. Fig. 46 Shows the cavitation development by pressure and acceleration spectrums. Where we can see the pressure spectrum is very smooth which means no detection of any vibration, in following chart some pulse of vibration are noted.

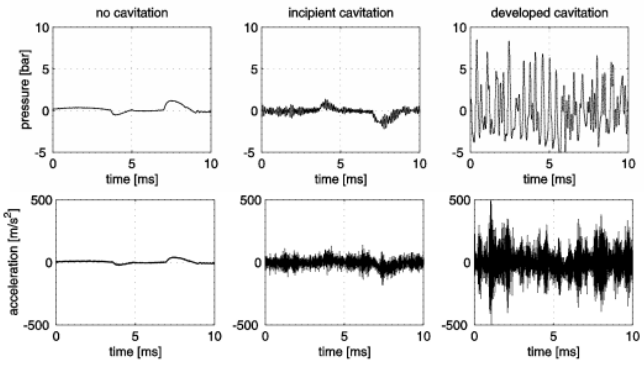

Fig.46: Vibration spectrum development [17].

D- **By monitoring of acoustic pressure emission [17]**

Cavitation usually produces high noise when the vapor bubbles got collapsed and high pressure peaks are generated. First bubbles collapse cannot be noted and audible by the human ears, developed stages of bubbles collapse can produce high and high noise so that human ear can hear it. By using some audio instruments like microphones and speakers we can record even the noise of inception cavitation.

E- By detection of Cavities by Flow Visualization [17]

Cavitation detection can be achieved by the flow visualization. Vapor bubbles can be detected visually in case the fluid is transparent.

4.4. Cavitation types [16]

As cavitation process defined previously, it is characterized by formation vapor bubbles. The fluid-vapor interaction could be with different shapes, according to that the cavitation can be classified.

Traveling cavitation: the vapor bubbles in this type are called cavitation nuclei, these nuclei are curried by the flow, and then they are growing during their flow before collapsing at higher pressure zones. The developed bubbles in complex shape are due to the interaction between them and the walls.

Attached cavitation: in contrast with the previous case, attached cavitation stays at same position of the bubbles formation. Attached cavitation doesn't mean the flow stays in the steady case because it is the mean source of unsteadiness.

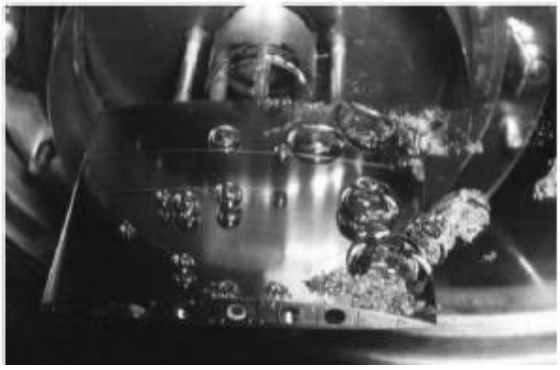

Fig.47: Traveling cavitation on suction side [17].

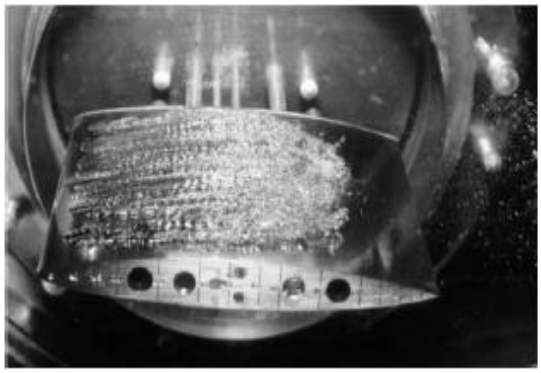

Fig.48: Attached cavitation on the foil Suction Side [17].

Vortex cavitation: this form of cavitation usually exist on the marine propeller, this type is generated by the secondary flow at the blade tip due to the pressure difference between both sides of the blade (suction and pressure)

Shear cavitation: this type of cavitation can be found in the wake of bluff bodies or in submerged liquid jets.

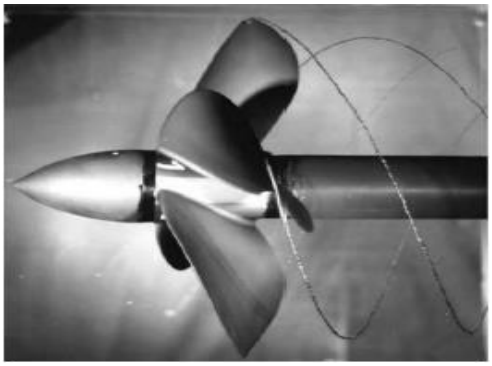

Fig.49: Vortex cavitation on the marine propeller [17].

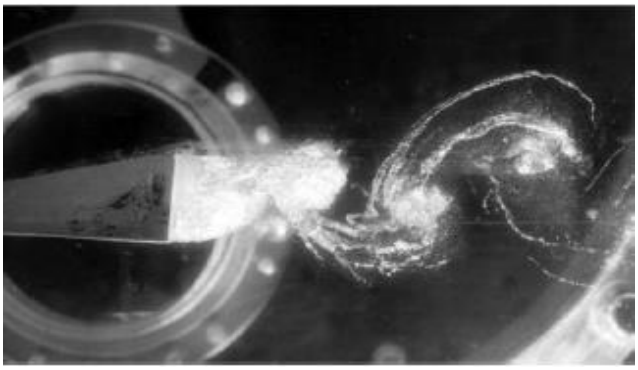

Fig.50: Shear cavitation in the wake of the bluff body [17].

4.5. Cavitation in centrifugal pump

As known from turbo machinery design, at the suction side of a blade in centrifugal pump, the rotation effect is imposed on the fluid, this effect increase the tangential velocity component increase the absolute velocity together with the axial velocity component and thus, decreasing of static pressure happens **[16]**.

The liquid inters the impeller eye going to leading edge of the blade to both sides, in case the suction side pressure is below the fluid vapor pressure, cavitation will be established and the vapor bubbles will curried by the flow to collapse at high pressure zones. As Fig. 31 shows, this happens only at high impeller speed and it is function of the flow velocity change, fluid properties, pressure gradient and the closeness to the pump walls.

The cavitation damage on the wall is like a sponge. Cavitation damage can be also found on the diffuser blades and the volute passage too. Because at the inception stage of bubbles formation, Collapsing occurs at the impeller wall but for developed stages, bubbles can move to different locations and collapse there.

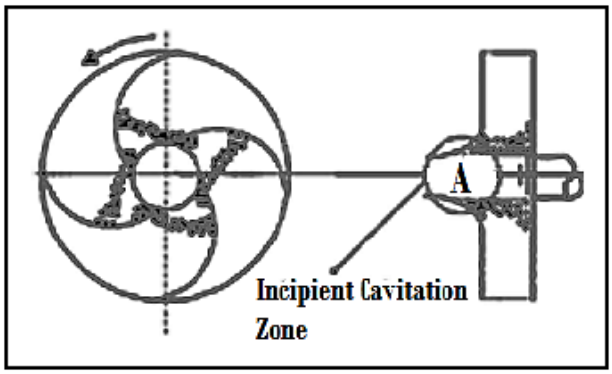

Fig.51: Most low pressure locations [16].

H. Ding [18], studied the performance of an axial pump with cavitation effect, Fig. 52 Shows the 3D CAD model geometry of the fluid zones. Where the fluid domain was divided into four sub-domains: inlet, rotor, stator and the outlet. Simulation was performed for the model with turbulence model k-ε and cavitation model too. Static pressure distribution on the surface of the axial pump is shown by Fig. 53.

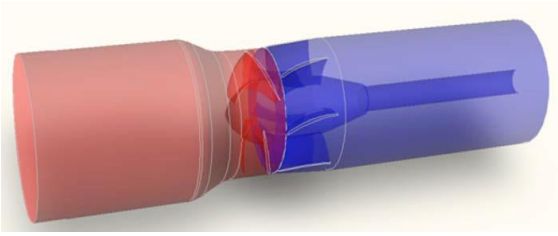

Fig.52: Axial pump model [18].

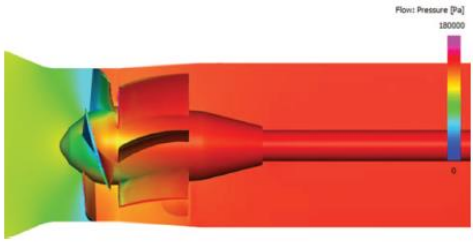

Fig.53: Static pressure disrtibution [18].

Fig. 54 Configurates the cavitation positions on the rotor blades with similarity in size and cavitation shape for all four blades in different flow rate, case (a) and (b). for case (c) and (d) the flow rate value was smaller and thus the cavitation area is smaller too.

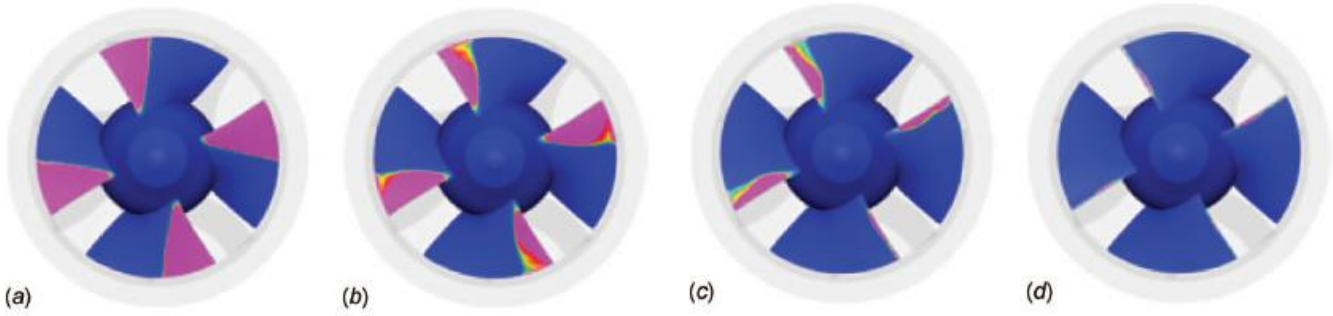

Fig.54: Cavitation area on an axial pump model [18].

4.6. Numerical simulation of firefighting pump model with cavitation model at the same boundary conditions

In order to investigate the bubbles formation for the simulated pump model, the simulation process was repeated with the same boundary conditions and the same inlet and outlet pressures for the highest speed which is 4200 rpm but, one modification has been done, cavitation model was included in multiphase system where, two phases were added to the model from fluent data base, water liquid and water vapor. Transfer mechanism from water liquid to water vapor was selected by cavitation, regardless to temperature changes, saturation temperature is set as the normal atmospheric condition which is 300 K., with vaporization pressure P_v is 3540 Pa as shown by Fig. 56

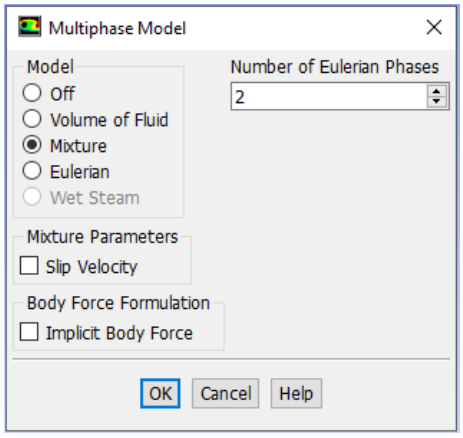

Fig.55: Multiphase model.

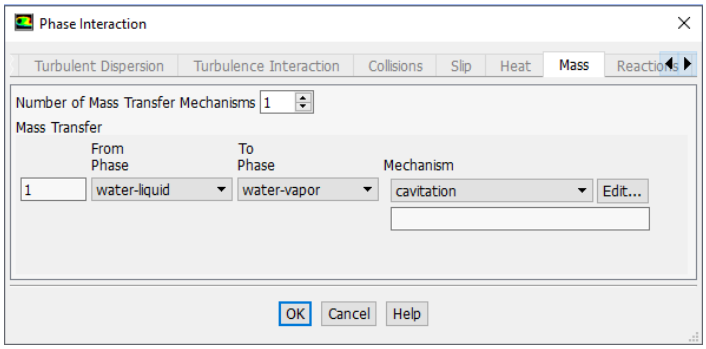

Fig.56: Phase change mechanism.

4.6.1. Simulation results

After finishing the simulation process, the results showed that, there is no vapor bubbles within all pump model which means, we won't get any cavitation at these operation condition, even if we increase the back presssure because according to Fig. 45 the worst case (when the cavitation is maximum), this happens at zero back pressure. Fig. 57 Illustrare the area of the liquid water phase which is 100%; in other words, there is no vapor bubbles (cavitation).

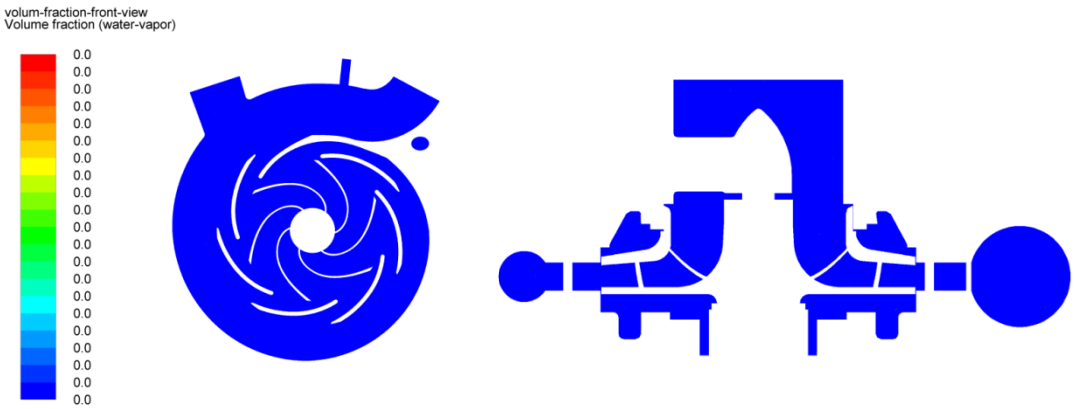

Fig.57: Vapor volume fraction from front and top view.

4.7. Numerical simulation of firefighting pump model with cavitation model but for different inlet pressure

As mentioned above, we got no cavitation at the previous condition and in order to check the cavitation areas, simulation process was repeated once more but with one change, inlet pressure was changed to -10 kPa instead -4 kPa. Simulation results showed that, cavitation areas exist in the low pressure zone within the pump geometry, where they are on suction side of impeller blades and on some position within the stator blades. In volute space cavitation hasn't appeared because the static pressure is much higher than bubbles formation pressure. Fig. 58 Illustrates the cavitation areas within the pump at four different back pressure, the maximum amount of the bubbles we can see at zero Pa and then, this amount got smaller and smaller till the back pressure reached 5 bar and cavitation disappeared.

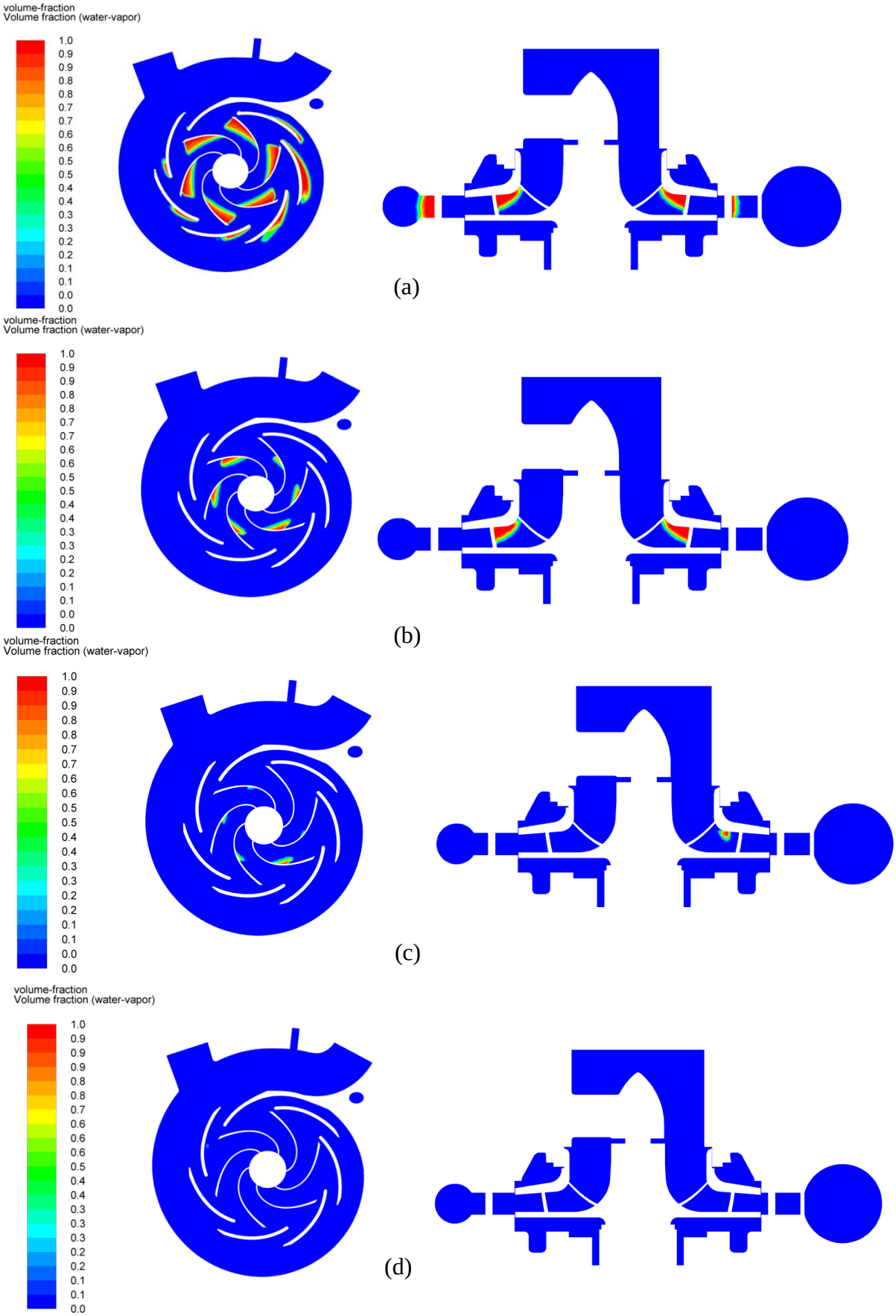

Fig.58: Cavitation areas at different back pressure value, (a) at 0 bar, (b) at 3 bar, (c) at 4 bar and (d) at 5 bar.

4.8. Performance of the pump model with cavitation presence

According to previous studies of centrifugal pump, cavitation presence affects the pump performance and its efficiency, mass flow rate and the head pressure decrease in case of presence of cavitation due to different specific volume between liquid water and vapor water and thus, the pump efficiency is reduced. Simulation of the pump model was run many times for different back pressure value. Table. (8) Shows the simulation results at new conditions with existing of vapor bubbles.

Table. 8: Pump characteristic according to latest simulation

Impeller speed = 4200 rpm				
Back pressure [bar]	**Mass flow rate [kg/s]**	**Inlet velocity [m/s]**	**Outlet velocity [m/s]**	**Inlet static pressure [kPa]**
0	41.435	4.91	7.36	-34.126
3	40.305	4.85	6.76	-32.671
4	38.067	4.76	6.28	-29.157
5	34.280	4.29	5.75	-28.475
6	29.384	3.73	4.58	-23.900
6.3	25.760	2.36	3.73	-15.591
6.4	0			

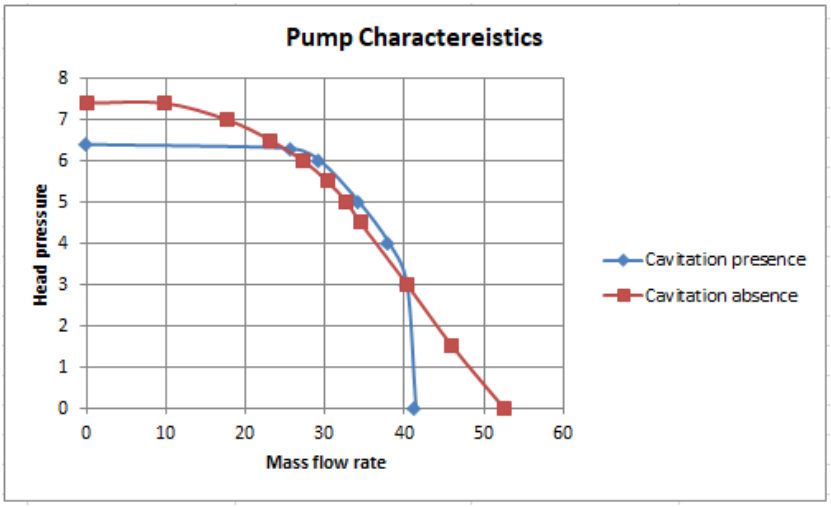

Fig.59: Pump characteristic in case of cavitation existing.

Similarly to Fig. 31 which showed the experimental pump characteristic at various impeller speed, there was a cavitation effect in the case of the high speed, Fig. 59 Shows also the effect of cavitation but by numerical method, deviation between presence and absence of cavitation is clear, cavitation causes a reduction in head pressure and flow rate of the pump too, this phenomenon reduces the pump efficiency because of these effects.

Cavitation inceptions is at a certain value of flow rate (almost 35 kg/s), where the head pressure curve deviates the optimal head curve and drops with straight line downward, that diagnoses the fault of the pump performance, and if the pump works continuously with increasing the capacity, the cavitation develops and leads to pump wall damage and other cavitation's effects.

4.9. Pump characteristic and its efficiency in case of cavitation existing

Based on equation. (39) hydraulic power is calculated and by the comparison between the hydraulic power and the consumed power, pump efficiency was calculated based on equation. (37) and illustrated by Fig. 60.

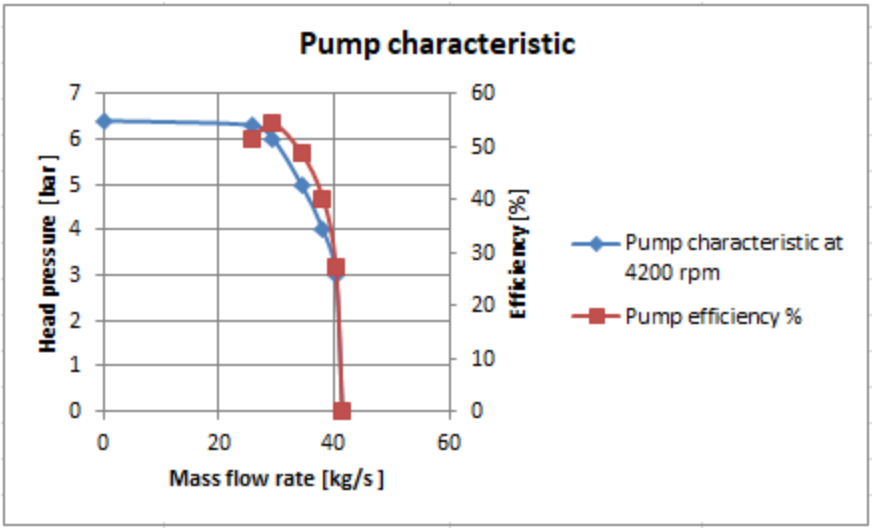

Fig.60: pump efficiency in case of cavitation presence

According to Fig .60 we can see the maximum efficiency is almost 55 % at 6 bar back pressure with approximately 30 kg/s as the flow rate, we can see the reduction in the pump efficiency from 61% when the pump operated at non-cavitation conditions to 55% in case of cavitation conditions, this confirms the effect of the cavitation and its damage. One more note we can see, the maximum efficiency we could obtained is at 6 bar as a back pressure in two cases presence/absence of cavitation, so this value is recommended to operate the pump at it.

Suggestions of pump design improvement

1- Improve the design of the impeller by using different outlet blade angle to give a highest efficiency, where based on [2] the best outlet blade angle is from 40 to 50 deg, our impeller outlet blade angle is 32 deg, to increase the hydraulic efficiency we need to modify the value of the outlet blade angle to located between 40 to 50 deg.
2- Increase the blades' number in order to get more transferred kinetic energy to pumped fluid, other way is also possible by using couple of rotors which almost gives double power to the pumped fluid but of course the impeller of the pump will need more power to be operated as well.
3- Reset the volute blades position to improve the smoothness of the flow, as we can see from Fig. 58 cavitation occurs between the volute blades too, this happens because of the flow direction between these blades, to prevent this phenomenon we need to make the flow smoother between them by modify the outlet angle, by increasing the angle, the flow will be more laminar and swirls will not be formed which prevent the pressure decreasing behind the blades
4- In case we want to increase the flow rate, forward impeller blades can be used instead of the backward but one disadvantage of this modification, the head pressure will be less than backward blades, in case we want to take the average value between the flow rate and the head pressure, we can use radial blades.
5- Increase the pressure at the inlet of the pump by using inducer.

One of the most effective method to reduce cavitation formation is to use an inducer, this inducer usually is installed at the upstream of the impeller. The main function of the inducer is to rise the inlet head pressure of the fluid to prevent significant cavitation in following pump stages. Is used in applications where the inlet pressure is close to vapor formation pressure of the pumped liquid. Inducers are frequently included in design of turbo pump machine. This tool allow us to operate the pump at higher rotational speed, which gives more economical operation case and higher efficiency. In order to create this inducer and for more understanding is to predict its hydraulic and dynamic characteristic. **Yao-jun [19]** Studied the presence of inducer in an axial pump, his pump model consists an inducer with three mounted blades on a conical hub, an impeller and diffuser. Main aim of the inducer is to guide the fluid smoothly into the impeller which provides the kinetic energy to the fluid.

Pump design parameters: impeller diameter is 0.3 m rotational speed is 1450, flow rate is 0.35 m^3/s. By using this device, static pressure in front of the impeller will not reach the vapor pressure. In other words, cavitation won't occurs. And thus, efficiency value will increase and the pump's life time will be longer.

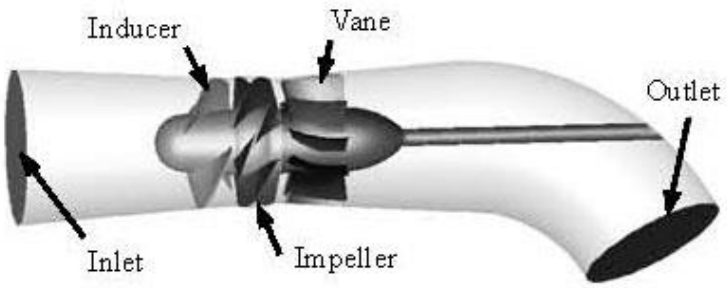

Fig.61: Pump model with inducer presence [19].

Conclusion

The study of a centrifugal pump performance has a great importance in order of analyzing the energy efficiency of the system. It is possible to conclude that as follow:

The mean difference between the efficiency pump and fire pump engine was explained and configured by a comparison between the performance of both of them and discussion their main difference and which parameter is more important in fire pump which was the flow rate at high back pressure, different parameter is more important for the efficiency pump which is the performance/efficiency of the pump. Effects of the outlet blade angle of the impeller blades was also explained on the pressure distribution within the pump and the velocity vector, also the effect of the number of impeller blades was also discussed, 7 and 10 blades gave the highest efficiency compared with the other cases. More explanation about the pump similarity law and the specific speed concept was included and the importance of the similarity laws and their formulas were discussed and included too.

An experiment on a firefighting pump was done in order to investigate the pump characteristic for different impeller speed, the comparison between them was illustrated and the effect of the variation impeller speed was explained.

Simulation for the firefighting pump model was done also to get more knowledge about the pump performance and compare the pump characteristic with the experiment results, for the simulation process, SST model under K-omega turbulence model was used as a turbulence model, this model is two-equation model. Boundary conditions were set at the inlet and the outlet as inlet and outlet pressure, Simulation process was run many time for different impeller speed with variation of back pressure value in order to get the pump characteristic, pressure and velocity contours too. Then the pump efficiency was calculated and compared with all cases, the results showed that, the highest efficiency is at the highest impeller speed at 6 bar back pressure which is the recommended operation condition to get the best performance by the pump.

Cavitation presence and the possibility of its existing within the pump geometry was also investigated, simulation process was run once more in order to investigate the cavitation presence but by using multiphase model in ANSYS software, where the liquid water and vapor

water were added to the model and the cavitation mechanism was selected and inlet pressure was set as -4 kPa. The results showed absence of the cavitation within all geometry of the pump.

In order to detect the possible areas of cavitation, the boundary condition at the inlet was changed to -10 kPa, all other parameters were maintained and simulation process was run for various back pressure at 4200 rpm, the results showed the cavitation areas within the pump geometry which are on the suction side of the impeller blades and some of them on the volute blades due to the flow deviation.

A comparison between the pump characteristic in presence and absence of cavitation was illustrated and discussed , and the pump efficiency with cavitation existing was calculated and illustrated with the pump characteristic, the results showed a reduction in the efficiency value from 61% to 55 % due to bubbles formation which causes to damage in the pump components.

References

1- Arnie Sdano, Boyko Tchavdarov and Denairic Hardersen, "**OPTIMAL FIRE PUMP DESIGN - CFD-AIDED REDESIGN OF A FIRE PUMP**", Proceedings of the ASME 2009 Fluids Engineering Division Summer Meeting, August 2-6, 2009.

2- E.C. Bacharoudis, A.E. Filios, M.D. Mentzos1 and D.P. Margaris, "**Parametric Study of a Centrifugal Pump Impeller by Varying the Outlet Blade Angle**", The Open Mechanical Engineering Journal, 2008, 2, 75-83.

3- G. Kergourlay,M. Younsi, F. Bakir, and R. Rey, "**Influence of Splitter Blades on the Flow Field of a Centrifugal Pump: Test-Analysis Comparison**", International Journal of Rotating Machinery, 21 November 2006.

4- José González, Jorge Parrondo, Carlos Santolaria and Eduardo Blanco," **Steady and Unsteady Radial Forces for a Centrifugal Pump With Impeller to Tongue Gap Variation**", JOURNAL OF FLUIDS ENGINEERING., September 29, 2005.

5- S.Chakraborty and K.M.Pandey, "**Numerical Studies on Effects of Blade Number Variations on Performance of Centrifugal Pumps at 4000 RPM**", International Journal of Engineering and Technology, Vol.3, No.4, August 2011.

6- A. J. Stepanoff, Ph.D., "Centrifugal and Axial Flow Pumps", Theory, Design, and Application, 1957.

7- K.M. Pandey, A.P. Singh, and Sujoy Chakraborty, "**Numerical Analysis of Centrifugal Pumps with Fluent Software**", International Journal of Applied Engineering Research ISSN, 0973-4562 Volume 6, Number 9 (2011).

8- J. C. Kuritza, G. Camponogara1, M. G. Marques, D. G. Sanagiotto and C. Battiston, "**Dimensionless curves of centrifugal pumps for water supply systems: development and case study**", Brazilian Journal of Water Resources, May 17, 2017.

9- P. TIMÁR, "**Dimensionless Characteristics of Centrifugal Pump**", 32nd International Conference of the Slovak Society of Chemical Engineering, Tatranské Matliare, 23—27 May 2005.

10- **Marius Stan, Ion Pana, Mihail Minescu, Adonis Ichim, and Catalin Teodoriu, "**Centrifugal Pump Monitoring and Determination of Pump Characteristic Curves Using Experimental and Analytical Solutions", JOURNAL OF FLUIDS ENGINEERING,13 February 2018.

11- Andrzej WILK, "**Hydraulic efficiencies of impeller and pump obtained by means of theoretical calculations and laboratory measurements for high speed impeller pump**

with open-flow impeller with radial blades", INTERNATIONAL JOURNAL OF MECHANICS, Issue 2, Volume 4, 2010.

12- Huimin Zhang1,a, Guangji Li1,b and Dongmei Peng, "The Influence of Speed on the Performance of Centrifugal Pump", Applied Mechanics and Materials Vols. 249-250 (2013) pp 512-516.

13- V. T. T Nguyen, s- Jun Kim, Y- Do Choi, "**EFFECT OF THE VOLUE TONGUE ON PERFORMANCE OF A CENTRIFUGAL PUMP WITH VERY LOW SPECIFIC SPEED**", Fluids Engineering Conference, July 26-31, 2015, Seoul, Kore.

14- Hamed Alemi, Seyyed Ahmad Nourbakhsh, Mehrdad Raisee and Amir Farhad Najafi, "**Effect of the volute tongue profile on the performance of a low specific speed centrifugal pump**", Journal of power and energy, , 23 October 2014.

15- Winterthur, Sulzer pumps, "**centrifugal pump handbook**", third edition 2010.

16- M. Binama, A. Muhirwa and E. Bisengimana, "**Cavitation Effects in Centrifugal Pumps**", Journal of Engineering Research and Application, Vol. 6, May 2016, pp.52-63.

17- Timo KOIVULA, "**CAVITATION IN FLUID POWER**", Institute of Hydraulics and Automatio, Hamburg 2000, pp. 371-382.

18- H. Ding, F. C. Visser, Y. Jiang and M. Furmanczyk, "**Demonstration and Validation of a 3D CFD Simulation Tool Predicting Pump Performance and Cavitation for Industrial Applications**", Journal of Fluids Engineering, JANUARY 2011, Vol. 13.

19- LI Yao-jun,and WANG Fu-jun, "**NUMERICAL INVESTIGATION OF PERFORMANCE OF AN AXIAL-FLOW PUMP WITH INDUCER**", Journal of hydrodynamic, June 25, 2007.